Redox Biology 41 (2021) 101925

Contents lists available at ScienceDirect

Redox Biology

journal homepage: www.elsevier.com/locate/redox

Crosslinking of human plasma C-reactive protein to human serum albumin via disulfide bond oxidation

Shuwen Jiang [a], Per Hägglund [a], Luke Carroll [a], Lars M. Rasmussen [b], Michael J. Davies [a,*]

[a] Department of Biomedical Sciences, Panum Institute, University of Copenhagen, Copenhagen, 2200, Denmark
[b] Center for Individualized Medicine in Arterial Diseases (CIMA), Department of Clinical Biochemistry and Pharmacology, Odense University Hospital, University of Southern Denmark, Odense, Denmark

ARTICLE INFO

Keywords:
Crosslink
Disulfide
Protein oxidation
C-reactive protein
Hypochlorous acid
Peroxynitrite
Aggregation

ABSTRACT

Inter- and intra-molecular crosslinks can generate protein dysfunction, and are associated with protein aggregate accumulation in aged and diseased tissues. Crosslinks formed between multiple amino acid side chains can be reversible or irreversible. Disulfides formed either enzymatically, or as a result of oxidant-mediated reactions, are a major class of reversible crosslinks. Whilst these are commonly generated via oxidation of Cys thiol groups, they are also formed by 'oxidant-mediated thiol-disulfide reactions' via initial disulfide oxidation to a thiosulfinate or zwitterionic peroxide, and subsequent reaction with another thiol including those on other proteins. This generates new intermolecular protein-protein crosslinks. Here we demonstrate that photooxidation, or reaction with the biological oxidants HOCl and ONOOH, of the single disulfide present in the major human plasma inflammatory protein, C-reactive protein (CRP) can give rise to reversible disulfide bond formation with human serum albumin (HSA). This occurs in an oxidant dose-, or illumination-time-, dependent manner. These CRP-HSA crosslinks are formed both in isolated protein systems, and in fresh human plasma samples containing high, but not low, levels of CRP. The inter-protein crosslinks which involve Cys36 of CRP and Cys34 of HSA, have been detected by both immunoblotting and mass spectrometry (MS). The yield of protein-protein crosslinks depends on the nature and extent of oxidant exposure, and can be reversed by dithiothreitol and tris(2-carboxyethyl) phosphine hydrochloride. These data indicate that oxidation of disulfide bonds in proteins can be a source of novel inter-protein crosslinks, which may help rationalize the accumulation of crosslinked proteins in aged and diseased tissues.

1. Introduction

Disulfide bonds between Cys residues on the same, or different, polypeptide chains are key stabilizing factors in folded proteins, and also in the formation of native protein multimers [1]. Native disulfides are formed via highly-regulated processes controlled by the ER oxidoreductin 1 (Ero1) and protein disulfide isomerase (PDI) families in the endoplasmic reticulum (ER) in eukaryotic systems, and disulfide oxidoreductase (DsbA) in the bacterial periplasm [2–4]. Disulfides can also be generated by oxidation of Cys residues, and via thiol-disulfide exchange reactions. The former involves oxidation of the thiol group (RS-H) to an intermediate RS-X (X = OH, NO, halogen, SCN), and subsequent reaction with a second thiolate anion (RS^-). These reactions are often rapid [5–8]. In contrast, direct reaction of RS^- with another disulfide (i.e. X = SR, 'thiol-disulfide exchange') is slow due to the small thermodynamic differences between starting materials and products [9,10]. Deliberate formation (engineering-in) of additional disulfide bonds has shown potential in extending the stability and activity of enzymes and protein-based therapeutics [11–15], so understanding the stability of these bonds and how they are modified by oxidants may contribute to the rational design of *de novo* disulfide bonds.

The formation of unintended disulfide bonds via oxidant reactions is typically counteracted by efficient reduction by cellular and extracellular enzymatic reducing systems (e.g. the thioredoxin and glutredoxin systems [16,17]). However, disruption of the balance between oxidant production and removal/repair pathways can result in the accumulation of modified materials [18,19]. This build-up, particularly of damaged proteins, is associated with aging and disease development [19–22]. There is significant variation in the redox potentials of different organelles, cells and fluids, with these systems not at equilibrium [23]. Thus some compartments are more oxidizing than others (e.g. the

* Corresponding author. Department of Biomedical Sciences, Panum Institute, Blegdamsvej 3, University of Copenhagen, Copenhagen, 2200, Denmark.
E-mail address: davies@sund.ku.dk (M.J. Davies).

https://doi.org/10.1016/j.redox.2021.101925
Received 2 February 2021; Received in revised form 26 February 2021; Accepted 26 February 2021
Available online 1 March 2021

Abbreviations

ACN	acetonitrile
CRP	recombinant human C-reactive protein
DTT	DL-dithiothreitol
FA	formic acid
HOCl	the physiological mixture of hypochlorous acid and its conjugate anion
HSA	human serum albumin
IAM	iodoacetamide
mCRP	monomeric human C-reactive protein
MB	methylene blue
nCRP	pentameric human C-reactive protein
NEM	*N*-ethylmaleimide
$^1O_2$	molecular oxygen in its lowest singlet excited state, $a^1\Delta_g$
OD	optical density
ONOOH	the physiological mixture of peroxynitrous acid and its conjugate anion
PBST	phosphate-buffered saline containing Tween 20
PDB	Protein Data Bank
RB	Rose Bengal
RF	riboflavin
TCEP	tris(2-carboxyethyl)phosphine hydrochloride
TFA	trifluoroacetic acid

endoplasmic reticulum, due to the requirements for disulfide bond synthesis and protein folding), and the extracellular milieu is typically more oxidizing than cellular organelles [23–25]. The redox potential of an environment helps determine the oxidation state of residues on proteins, and particularly the cysteine/cystine (thiol-disulfide) couple, and hence the activity and function of proteins [26]. Perturbation of these couples can result in higher levels of disulfides or other oxidized thiol species, relative to reduced thiols [24,25].

Serum albumin (HSA) is the most abundant human plasma protein, accounting for ~50% of the total protein load and ~80% of the thiol content [27,28]. Native HSA contains 17 disulfides, and a single free Cys (Cys34) which is readily modified by oxidants and electrophiles [29,30]. The percentage of Cys34 that is present in its native (reduced) form, in healthy human plasma, is typically ~70%, with the remainder present as oxidized forms (including sulfenic, sulfinic and sulfonic acids, nitrosylated species, mixed dimers with other thiols, and adducts with nucleophiles (e.g. quinones and unsaturated aldehydes) [31–35]. Increased levels of these modified forms are associated with smoking, aging, and multiple acute and chronic diseases [36–39].

In recent studies we have shown that oxidant-mediated disulfide exchange reactions can be rapid [40–44] especially when compared to 'normal' thiol-disulfide exchange reactions [9,10]. Initial disulfide oxidation with multiple oxidants including HOCl, HOBr, HOSCN, ONOOH, H_2O_2, peracids and $^1O_2$ yields a reactive thiosulfinate [RS-S(=O)R] or zwitterion peroxide [RS-S^+(-OO^-)R] [40–42,45–48]. The rate constants for these reactions depend on both the oxidant, and the structure and conformation of the disulfide [40,45].

Thiosulfinates or zwitterion peroxides have modest lifetimes (~hours, depending on their structure [42,44]) and can undergo subsequent reaction with both low-molecular-mass thiols (e.g. GSH and N-acetylcysteine) to give thiolated/glutathionylated products [41,42,44], and also thiol groups on another protein to yield protein-protein disulfide bonds [43]. These 'oxidant-mediated thiol-disulfide exchange reactions' provide a novel pathway to glutathionylated proteins and protein crosslinks, and particularly for proteins that do not contain an initial free Cys residue.

These reactions cleave the original disulfide, and therefore impact adversely on protein structure and function [43]. They have also been detected in human plasma indicating that these reactions are kinetically-competent, even in the presence of other targets [42,44]. These data indicate that disulfide oxidation can be facile, and is potentially important. For extracellular fluids and proteins, such oxidation is likely to be enhanced by the high abundance of disulfides compared to other targets in HSA (cf. the data given above), and extracellular matrix proteins, receptors and ligand-binding proteins (cf. the ~200 disulfide bonds in laminin proteins). Modification of some extracellular disulfides appears to be *functionally* important, with cleavage (by poorly-defined mechanisms) of disulfide bonds in plasminogen and von Willebrand factor (VWF) resulting in conformational changes and oligomer formation [49,50].

Acute and chronic inflammation is typically associated with dramatic elevations in acute phase proteins, including C-reactive protein (CRP). The latter can be detected at levels up to 10,000-fold higher than controls, and this is widely used as a biomarker of inflammation and disease severity (e.g. in cardiovascular syndromes, type 2 diabetes, pancreatitis, meningitis, cholecystitis), and prognosis (reviewed [51,52]). CRP is a homo-pentameric protein, with each non-covalently associated subunit consisting of 206 amino acids with one internal (intra-subunit) disulfide bond (Cys36-Cys97). This serves as a redox-sensitive switch that controls the structure and biological properties of the protein [53,54]. Pentameric CRP (nCRP) is irreversibly dissociated to its monomeric form (mCRP) at sites of inflammation, with both species having biological effects [52]. A previous study [55] has shown that CRP can be modified by the oxidant hypochlorous acid (HOCl), generated by the heme enzyme myeloperoxidase (MPO) [56], with the level of the latter strongly associated with tissue damage and disease (reviewed [56–59]). HOCl modification results in protein unfolding and products that are potent platelet activators [55]. The mechanisms underlying these changes are poorly understood, but reduction or mutation of the Cys residues of the CRP disulfide bond results in protein unfolding, and the release of interleukin-8 and monocyte chemoattractant protein-1 from human coronary artery endothelial cells [54]. Disulfide-reduced mCRP is also a potent upregulator of adhesion molecule expression, and induces cytokine release from rabbit arteries *ex vivo* and in mice [54]. mCRP can also induce nitric oxide ($NO^{\cdot}$) generation with consequent vasodilation [60]. Thus, CRP is not only a marker, but also a *driver* of inflammation, with disulfide bond modification having functional, signaling and pro-inflammatory effects.

In the light of this data we hypothesized that oxidation of the mCRP disulfide bond would result in formation of zwitterionic peroxides or thiosulfinate species (depending on the oxidant), protein unfolding, and potential reaction of these species with other plasma proteins to form inter-protein disulfide crosslinks and protein aggregates. Such crosslinked species may serve as a biomarker for inflammation-induced damage in disease.

2. Materials and methods

2.1. Materials

Recombinant human C-reactive protein (CRP) was obtained from Lee Biosolutions (Maryland Heights, MO, USA). Human serum albumin (HSA), Rose Bengal (RB), riboflavin (RF), Coomassie brilliant blue G, *N*-ethylmaleimide (NEM), tris(2-carboxyethyl)phosphine hydrochloride (TCEP), DL-dithiothreitol (DTT), iodoacetamide (IAM) and catalase from bovine liver were purchased from Sigma Aldrich (Søborg, Denmark). Sequencing grade trypsin and Glu-C were purchased from Promega (Nacka, Sweden). Anti-CRP antibody (ab32412) and a human CRP ELISA kit (ab260058) were obtained from Abcam (Cambridge, UK). Human serum albumin monoclonal antibody (KT11), NuPAGE MES SDS running buffer (20×), NuPAGE LDS sample buffer (4×), NuPAGE 4–12% Bis-tris gels and NuPAGE reducing reagent (10×), were obtained from

Thermo Fisher (Hvidovre, Denmark). Sheep anti-mouse IgG HRP-linked whole Ab (NXA931-1ML), methylene blue (MB), trifluoroacetic acid (TFA), ammonium bicarbonate, acetonitrile (ACN) and formic acid (FA) were obtained from VWR (Søborg, Denmark). Anti-rabbit IgG HRP-linked antibody was obtained from Cell Signaling Technology (Danvers, MA, USA). All solvents employed were HPLC grade. Human plasma samples (heparin-treated) were obtained fresh as excess materials from individuals undergoing routine clinical chemistry analysis at the Department of Clinical Biochemistry and Pharmacology, Odense University Hospital. Samples were completely anonymized without any data on age, gender or other clinical information regarding the donors.

2.2. Protein oxidation

For photolysis experiments, purified CRP (5 μM) and plasma samples (2 mg protein mL^{-1}) were prepared in 10 mM phosphate buffer (pH 7.4), a photo-sensitizer (10 μM RB, 35 μM RF or 50 μM MB) was added, and the samples illuminated through a $\lambda > 345$ nm cut-off filter, in the presence of O_2 for different time points using a Leica P 150 slide projector. After photolysis, catalase (1 mg mL^{-1}) was added to the reaction system to remove photogenerated H_2O_2. Control samples, where protein or plasma samples were exposed to visible light alone (without photosensitizers), or where the protein samples or plasma samples were incubated with photosensitizers for similar periods with no light exposure, were also prepared and examined.

Stock solutions of HOCl and ONOOH were prepared in 0.1 M NaOH buffer and quantified spectrophotometrically as reported previously (HOCl, $\varepsilon_{292\ nm}$ 350 M^{-1} cm^{-1}; ONOOH, $\varepsilon_{302\ nm}$ 1705 M^{-1} cm^{-1}) [61,62]. For HOCl- and ONOOH- induced oxidation experiments, purified CRP (5 μM) and plasma samples (2 mg protein mL^{-1}) were incubated with HOCl (5 μM, 50 μM, 500 μM and 1000 μM) for 1 h, or with ONOOH (2.5 μM, 5 μM, 50 μM and 250 μM) for 30 min at 21 °C. Protein or plasma samples incubated for the same period with buffer in place of the oxidants (HOCl and ONOOH) served as controls.

2.3. SDS-PAGE and immunoblotting

For the analysis of protein crosslinks, SDS-PAGE was performed using NuPAGE 4–12% precast polyacrylamide gel with MES buffer under non-reducing or reducing conditions. Protein or plasma samples were mixed with non-reducing (10 mM phosphate buffer) or reducing sample buffer (NuPAGE reducing agent, Thermo; containing a final concentration of 50 mM dithiothreitol, pH 8.5) and heated at 60 °C for 10 min with NuPAGE LDS sample buffer, prior to electrophoresis at 200 V for 35 min. After electrophoresis, gels were either stained with Coomassie brilliant blue, or transferred onto a polyvinylidene fluoride membrane (PVDF) using an iBlot 2 system as described by the manufacturer (Thermo Fisher). Blots were incubated with 5% skim milk containing 2.5 mM NEM on a platform rocker for 1 h at 21 °C, followed by incubation with primary antibodies (anti-CRP antibody: 1:5000, anti-HSA antibody: 1:5000, both diluted in in PBS buffer supplemented with 1% Tween (PBST) at 4 °C overnight. After washing, the membranes were incubated with secondary anti-rabbit-HRP or anti-mouse-HRP conjugates (1:5000, diluted in 1% PBST) for 1 h at 21 °C. Chemiluminescence (ECL plus solution) was analyzed using an Azure Biosystems imager (AH Diagnostics, Aarhus, Denmark). Quantification of protein bands was performed using Image J software (NIH, USA).

2.4. ELISA measurement

A commercial ELISA assay from Abcam (see above) was used to quantify human CRP in solutions, or CRP levels in plasma samples before and after photo-oxidation (as described above, with the samples then transferred to ELISA plates). In brief, 100 μL of plasma samples with high CRP levels (diluted to 80 ng protein mL^{-1}) or purified CRP [diluted to the concentration of CRP determined in healthy (low CRP), plasma samples, ~300 pg mL^{-1}] were added into each well of the 96-well ELISA plate and incubated for 2 h at 21 °C, followed by treatment with the supplied biotinylated CRP antibody and HRP-streptavidin solution according to the manufacturer's instructions. After addition of the stop solution, the optical density was immediately measured at 450 nm on a microplate reader (SpectraMax® i3, Molecular Devices).

2.5. Protein identification using LC-MS/MS

Gel processing and in-gel digestion was performed according to a previously described method with minor modifications [63]. Briefly, gel slices containing the chosen protein bands (e.g. CRP, HSA and CRP-HSA crosslinked bands) were cut from the Coomassie-stained and washed SDS-PAGE gels. The gel sections were then dissected into 1 x 1 mm pieces, de-stained and subsequently reduced with DTT (50 mM) and alkylated with IAM (200 mM), followed by dual enzyme in-gel digestion. In general, the bands extracted from the same position in the gel were divided into two sets. One set was used for the detection of CRP, with trypsin (13 ng μL^{-1}) and subsequently Glu-C (13 ng μL^{-1}) used for proteolytic digestion, with both enzymes added to the in-gel samples. The second set was used for detection of HSA, with proteolytic digestion carried out using trypsin (22 ng μL^{-1}) and subsequently Glu-C (13 ng μL^{-1}) with both incubations carried out at 37 °C overnight. At the end of the digestion period, the gel pieces in each vial were mixed with 5% FA in ACN and shaken for 15 min. The extracted peptides were purified using a custom-made C18 StageTip before nanoLC-MS/MS analysis.

After drying using a Speedvac concentrator at 30 °C, peptide samples were reconstituted with 0.1 % FA and analyzed on an Impact II Q-TOF mass spectrometer (Bruker, Bremen, Germany) coupled to a Dionex Ultimate 3000RS nano chromatography system (Thermo, Waltham, MA, USA). The samples were eluted using a gradient system consisting of mobile phase A (0.1% FA in H_2O) and B (80% ACN containing 0.1% FA in H_2O). Peptide separation was performed using a Nanoelute C18-reversed phase column (75 μm × 15 cm, 1.9 μm particle size, Bruker, Bremen, Germany) at a flow rate of 0.3 μL min^{-1} with a gradient as follows: ramp from 5% B at 4 min to 61% B at 35 min, ramp to 99% B over 5 min, hold for 5 min, and ramp back to 4% B over 10 min. The temperature of the drying gas was set at 180 °C with a flow rate of 4 L min^{-1}. MS and MS/MS spectra were acquired in the positive ionization mode with acquisition rate of 2 Hz (MS) and 2.03 Hz (MS/MS). The MS data was acquired over a mass range of 150–1750 m/z, followed by MS/MS scans of the top 10 most intense precursor ions per cycle.

Protein identification was accomplished using the MaxQuant (version 1.6.1.0; www.maxquant.org) search engine with the following parameters: carbamidomethylation of Cys (fixed modification); Met oxidation (variable modification); allowed number of missed cleavages, 3; first search mass tolerance, 0.07 Da; main search peptide tolerance, 0.006 Da. Peptides were searched against the following UniProt protein accession numbers: human C-reactive protein P02741; HSA: P02768.

2.6. Mass spectrometric analysis of protein crosslinks in solution

For the identification of crosslinks between CRP and HSA, in solution digestion of protein mixtures was performed on samples that were treated with IAM (final concentration: 50 mM) either without reduction, or with reduction and alkylation using DTT/IAM after digestion. Briefly, protein samples (20 μg) which has been dried down in a Speedvac were redissolved and denatured in urea buffer (8 M urea, 50 mM Tris-HCl, pH 8), and the alkylating reagent IAM (final concentration: 50 mM) was added into the system to block free thiols on HSA. The concentration of urea was then diluted to 1 M with 100 mM ammonium bicarbonate, trypsin was added to achieve a 1:50 (w/w) enzyme/substrate ratio, and the reaction mixtures were incubated at 37 °C overnight. After digestion, the samples were either examined directly or subjected to reduction and alkylation to cleave the new disulfide and alkylate the resulting thiols. The latter was achieved by treating the samples with DTT (40 mM in

100 mM ammonium bicarbonate, pH 8.0) for 45 min, followed by incubation with IAM (100 mM in 100 mM ammonium bicarbonate, pH 8.0) for 60 min in the dark.

Peptide samples purified using custom-made C18 StageTips were analyzed on an Impact II Q-TOF mass spectrometer (Bruker, Bremen, Germany) coupled to a Dionex Ultimate Capillary-Flow LC system (Thermo, Waltham, MA). Peptides were loaded onto a Proswift RP 4H Monolithic Capillary column (200 μm ID x 25 cm) and eluted over 35 min at 35 °C using a gradient elution system consisting of mobile phase A (0.1% FA in H_2O) and B (80% ACN in H_2O containing 0.1% FA) at a flow rate of 10 μL min^{-1}. A linear gradient was used consisting of: 5% B over 3 min, ramped to 60% B over 12 min, ramped to 95% B over 3 min and hold constant for 9 min, and then ramped back to 5% B over 1 min, and re-equilibration in 5% B for 7 min until the end of the run. The operation conditions for the ESI source were as follows: capillary, 4.5 kV; dry heater, 250 °C, and dry gas 4.5 L min^{-1}. A high resolution TOF-MS scan over a mass range of 300–3000 *m/z* was followed by MS/MS scans of the top 3 most intense precursor ions per cycle. The preferred charge state range was set to 4–7.

The MassAI software (University of Southern Denmark, version 1.0) was used for identification of disulfide-linked peptides with the following settings: variable modification (Met oxidation); basic cross-linking: C–C (-2.016 Da); maximum number of missed tryptic cleavages, 2; parent mass tolerance, 20 ppm; MS2 peak tolerance, 0.2 *m/z*. GPMAW software version 9.5 (Lighthouse Data) was used for validation of fragmentation patterns of potential cross-linked peptides. Peptides were searched against the following UniProt protein accession numbers: human C-reactive protein, P02741; HSA, P02768.

2.7. Statistics

Data are presented as means ± standard deviations from at least three independent experiments. Statistical analyses were carried out using the statistical package GraphPad Prism version 6 (La Jolla, USA) by one-way analysis of variance (ANOVA) with Dunnett's multiple comparison test. Statistical significance was assumed at the $P < 0.05$ level.

3. Results

3.1. Photooxidation results in damage to both isolated CRP, and CRP in human plasma

Recombinant human purified CRP, and human plasma samples with high CRP levels, were subjected to photooxidation induced by illumination, for varying periods of time, with visible light in the presence of the photosensitizing dye RB and molecular oxygen (O_2). This system generates high yields [64,65] of the potent oxidant, singlet oxygen ($^1O_2$) which reacts rapidly with proteins, and particularly sulfur-containing (Cys, Met, cystine) and aromatic (Trp, Tyr, His) amino acids (reviewed [66,67]). Such oxidant exposure resulted in an illumination-time dependent loss of recognition by a native protein mAb of the monomeric form of the protein (mCRP, molecular mass ~23 kDa), in both immunoblotting and ELISA experiments (Fig. 1). Thus, exposure of isolated CRP (~1 μg mL^{-1} in 10 mM phosphate buffer, pH 7.4) to the complete photooxidation system resulted in a rapid depletion of the monomer band detected in immunoblotting experiments, with a significant loss of band intensity detected after 5 min of illumination, and almost complete loss at 15 min (Fig. 1A, C). Incubation of the protein with RB in the absence of light showed no loss of recognition (data not shown), and exposure of the protein to visible light in the absence of the sensitizer, did not result in a significant loss of band intensity (Fig. 1A, lane 2). Exposure of fresh human plasma (from donors with high CRP levels, diluted to give a similar CRP concentration to the isolated protein experiments) to a similar oxidative insult resulted in less dramatic changes in the recognition of the protein band by the anti-CRP antibody as detected by immunoblotting (Fig. 1B, D), but significant losses in recognition at longer illumination times in ELISA experiments (Fig. 1E). These changes were not detected in the absence of light, or the absence of RB (Fig. 1E). The less extensive loss of the CRP signal detected with the plasma samples when compared with the isolated system, containing similar concentrations of CRP, is ascribed to the presence of large

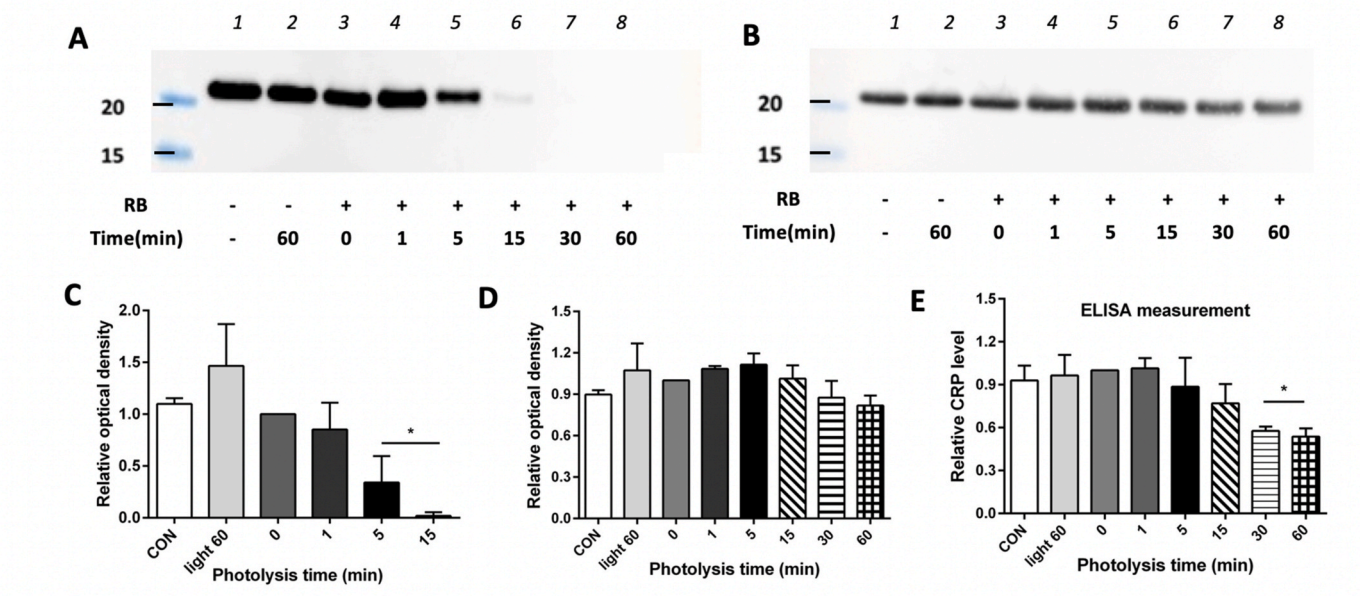

Fig. 1. Detection of CRP levels in solution samples and plasma upon exposure to $^1O_2$. Panels A and B: Representative immunoblotting images of monomeric CRP after photolysis of purified CRP (~1 μg mL^{-1}) in phosphate buffer, and diluted plasma (protein concentration: 0.2 mg mL^{-1}, containing CRP at 0.73–0.86 μg mL^{-1}), respectively, as detected using an anti-CRP antibody. Panel C: Optical density ratio ($OD_{lane\ n}/OD_{lane\ 3}$) of CRP bands presented in panel A (n = 1 min, 5 min and 15 min). Panel D: Optical density ratio ($OD_{lane\ n}/OD_{lane\ 3}$) of CRP bands presented in panel B (with n = 1, 5, 15, 30 or 60 min). Panel E: ELISA measurement of CRP levels detected in plasma (donors with high CRP level, ~300 pg mL^{-1}) after photolysis for different time points. Statistical differences are indicated as follows: *$P < 0.05$ vs. samples at 0 min photolysis time. Error bars represent SD of at least three independent experiments.

numbers of other proteins in the plasma samples which would be expected to act as alternative and competing targets for $^1O_2$.

3.2. CRP-HSA crosslinks are formed on incubation of RB-oxidized CRP with HSA or fresh human plasma

As previous data has shown that disulfides yield zwitterion peroxides on reaction with $^1O_2$ [68,69], and we have recently demonstrated reaction of these species with other thiols to give new thiolated proteins at the site of the original disulfide [42,44], we examined whether similar reactions can occur between photooxidized CRP and plasma proteins. Evidence for these reactions was sought by illuminating the CRP in the presence of RB and O_2, and then, after cessation of the illumination, addition of either purified HSA, or diluted fresh human plasma (with low CRP levels), with analysis of the samples carried out by separation of the proteins by SDS-PAGE, and subsequent immunoblotting with both anti-CRP and anti-HSA antibodies. Thus CRP (5 μM) was illuminated with visible light/RB/O_2 for different time points then reacted with HSA (5 μM) or diluted plasma (total protein concentration: 2 mg mL^{-1}) with low CRP levels (<100 ng mL^{-1} compared to HSA 0.7–1.2 g L^{-1}) for 1 h.

Immunoblotting analyses using an anti-CRP antibody showed the presence of photo-generated dimers of CRP, with the extent of dimerization increasing with longer photolysis times over the period 5–30 min (Fig. 2A). These species were not observed, but likely to be present, with the much lower levels of CRP used in the experiments reported in Fig. 1. Low levels of dimers were detected in control samples (Fig. 2A, lane 1). Similar levels of CRP dimer were detected after illumination for 30 min in the absence of RB (Fig. 2A, lane 2). Treatment of parent (non-oxidized CRP) with HSA, with subsequent probing with the anti-CRP antibody did not result in the detection of any additional immuno-reactive species (Fig. 2A, lane 4). Similarly, treatment of CRP which had been exposed to light for 30 min in the absence of RB, and then incubated with HSA, did

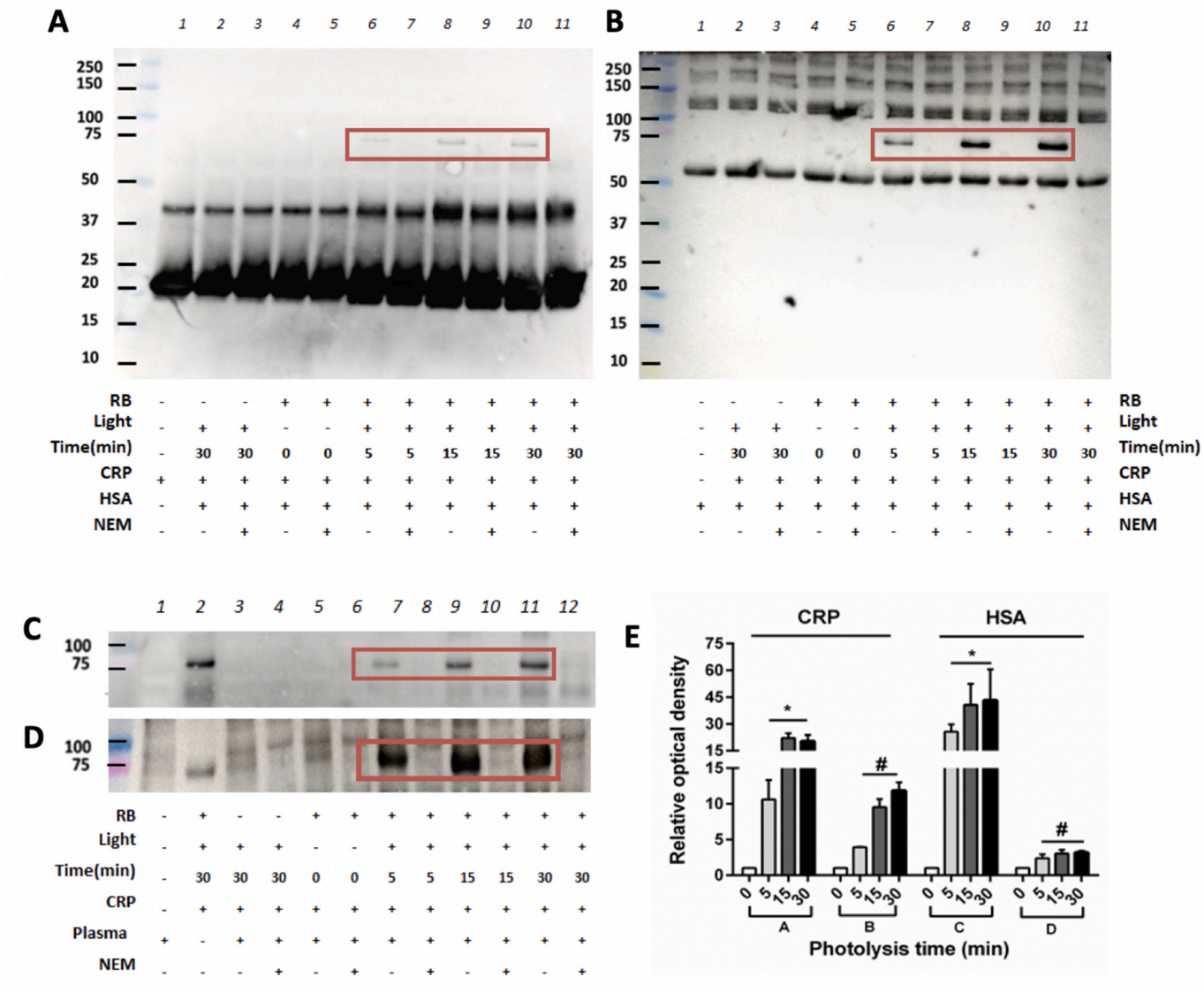

Fig. 2. Formation of CRP-HSA crosslinks on exposure of purified CRP to $^1O_2$ and subsequent reaction with HSA or plasma, and analysis by immunoblotting. Panels A and B: Formation of CRP-HSA crosslinks between oxidized CRP and HSA, as detected using an anti-CRP antibody and an anti-HSA antibody, respectively. Panels C and D: CRP-HSA crosslinks formed between oxidized CRP and plasma (2 mg protein mL^{-1}, HSA: 0.7–1.2 g L^{-1}), with detection by an anti-CRP antibody and an anti-HSA antibody, respectively; Lane 2 served as the positive control (reaction between oxidized CRP and purified HSA). Panel E: Optical density ratio ($OD_{n\ min}/OD_{0\ min}$) of crosslinked bands from immunoblotting data presented in panels A–D (with n = 0, 5, 15 or 30 min): A and C are OD ratios from panels A and B, respectively; B and D are OD ratio from panels C and D, respectively. Statistical differences are indicated as follows: *$P < 0.05$ vs. lane 4 (panels A and B), $^{\#}P < 0.05$ vs. lane 5 (panels C and D). Error bars represent SD of at least three independent experiments.

not give additional bands (Fig. 2A, lane 2). However, treatment of CRP which had been subjected to the complete photooxidation system for increasing time periods, and then exposed to HSA for 1 h resulted in the detection at an additional band at ~75 kDa (indicated by red box in Fig. 2A), which increased in intensity with greater extents of pre-oxidation of the CRP (Fig. 2A, lanes 6, 8, 10). The mass of this band is consistent with the presence of a CRP-HSA crosslink.

Probing of identical membranes with an anti-HSA antibody showed the presence of the parent HSA (which runs at an apparent molecular mass of ~55 kDa on these non-reducing gels) together with dimers and higher aggregates (Fig. 2B, lane 1). As expected, inclusion of CRP treated with visible light in the absence of RB, or the complete reaction system with no light exposure, did not result in significant changes. However, when photooxidized CRP was included, an additional band at ~75 kDa was detected (Fig. 2B, lanes 6, 8, 10; indicated by red box). This species runs at an identical mass to the additional species observed with the anti-CRP antibody, and is therefore assigned to a CRP-HSA crosslink. The intensity of this band increased with longer initial photooxidation times of the added CRP. Densitometric analysis of the membranes probed with the anti-CRP and anti-HSA antibodies (i.e. Fig. 2, panels A, B) showed a ~19-fold and ~42-fold increase in the intensity of the cross-linked band for the 30 min RB-illuminated samples relative to 0 min RB-illuminated samples, as detected by anti-CRP and anti-HSA antibody, respectively (Fig. 2E).

A similar pattern of behavior was observed when fresh human plasma was incubated with photooxidized CRP, with the membranes then probed with either an anti-CRP antibody (Fig. 2C) or the anti-HSA antibody (Fig. 2D), though the overall intensity of the bands was weaker. Densitometric analysis showed a similar increase in the band from the proposed CRP-HSA crosslinked species, with significant increases in pixel intensity seen with both antibodies with increasing photolysis time of the original CRP (Fig. 2E).

The potential role of the Cys34 thiol group present on HSA, and also thiols present on other plasma proteins, in these reactions was examined using samples prepared in an identical manner to those described above, except that the isolated HSA (5 μM, as above) or plasma (2 mg protein mL^{-1}, as above) were pre-treated with the thiol-blocking reagent *N*-ethylmaleimide (NEM, 10-fold molar excess over the purified CRP concentration, 1 mM for plasma sample, for 1 h at 37 °C) prior to addition to the pre-oxidized CRP samples. This pre-treatment of the HSA or plasma, significantly inhibited the formation of the CRP-HSA crosslinks (Fig. 2A, B, lanes 7, 9, 11 versus 6, 8, 10; Fig. 2C, D, lane 8, 10, 12 versus 7, 9, 11). These data establish that the new species with apparent molecular mass of ~75 kDa, requires the presence of pre-oxidized CRP and a free Cys residue on the added HSA or plasma proteins, and that this species is not formed in the absence of pre-oxidation of the CRP (i.e. is not formed via 'traditional' thiol-disulfide exchange reactions).

3.3. Detection of CRP-HSA crosslinks on exposure of plasma to photooxidation

As the systems described above are artificial in that the thiol-containing species (HSA or plasma) was added to the CRP *after* the latter was oxidized, further experiments were carried out with plasma that contained either low or high levels of CRP with the photooxidation carried out directly on the samples. Thus, the possible formation of inter-

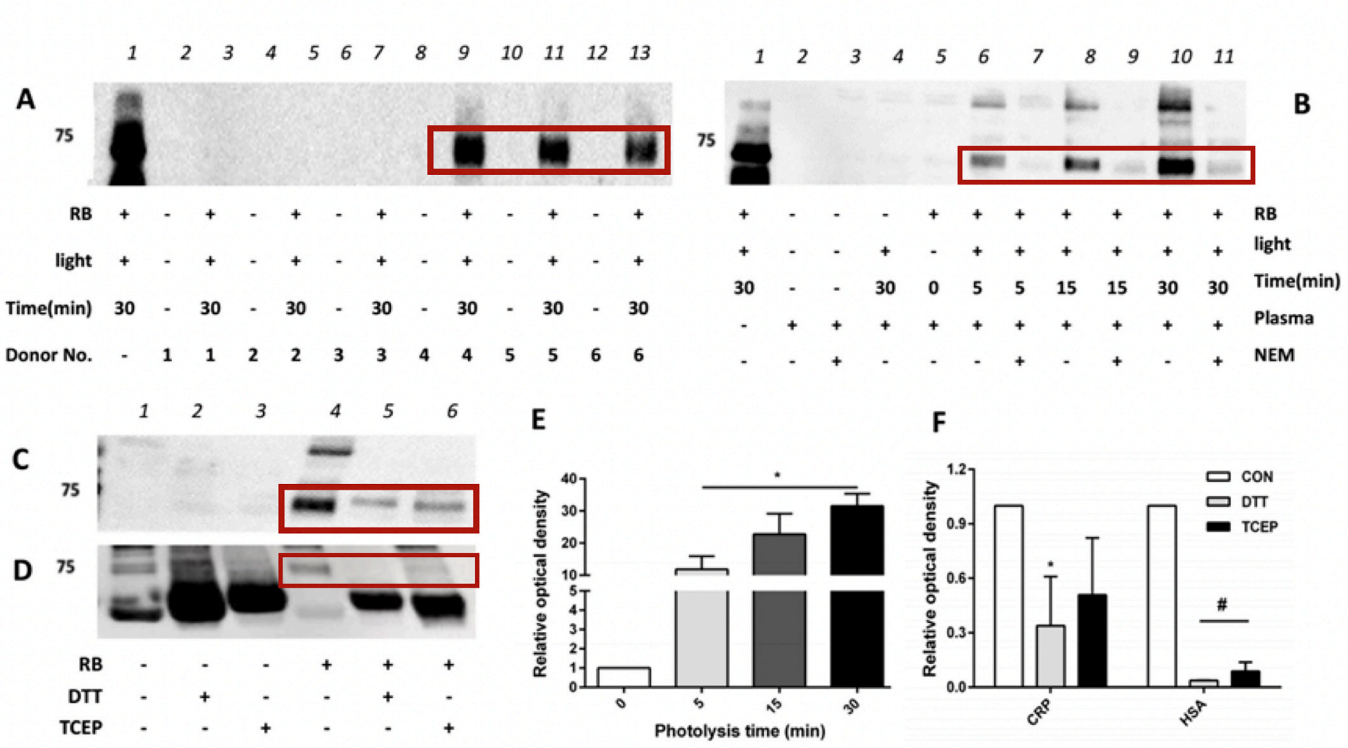

Fig. 3. Immunoblotting detection of CRP-HSA crosslinks formed in plasma as a consequence of RB-induced photolysis. Panel A: Detection of CRP-HSA crosslinking in plasma samples from six donors (lane 2–7 were from three donors with CRP levels < 100 ng mL^{-1}; lane 8–13 were from three donors with high CRP level: 7.3–8.6 μg mL^{-1}), as detected using an anti-CRP antibody. Panel B: Time-dependent formation of CRP-HSA crosslinking in plasma samples (donors with high CRP level) after photolysis, as detected by immunoblotting using an anti-CRP antibody; In panels A and B, lane 1 served as the positive control (reaction between oxidized CRP and HSA). Panels C and D: Reduction of CRP-HSA crosslinks by treatment with the reducing agents DTT/TCEP, as detected by immunoblotting using an anti-CRP antibody and an anti-HSA antibody, respectively. Panel E: Optical density ratio ($OD_{n\ min}/OD_{0\ min}$) of the CRP-HSA crosslinking bands presented in panel B (with n = 0, 5, 15 or 30 min). Panel F: Optical density ratio ($OD_{DTT\ or\ TCEP}/OD_{con}$) of crosslinked protein bands presented in panels C and D. Statistical differences are indicated as follows: *P < 0.05 vs. lane 5 (panel B) or * P < 0.05 vs. lane 4 (panel C), #P < 0.05 vs. lane 4 (panel D). Error bars represent SD of at least three independent experiments.

molecular CRP-HSA crosslinks was examined by subjecting plasma samples from six donors, three with high CRP levels (7.3–8.6 μg mL^{-1}) and three with low CRP levels (<100 ng mL^{-1}) to photooxidation. Exposure of plasma that contained high CRP levels (Fig. 3A, donors 4, 5, 6) to visible light in the presence of RB/O_2 resulted in the detection, using the anti-CRP antibody, of the band at ~75 kDa assigned to the CRP-HSA crosslink (Fig. 3A, lanes 9, 11, 13). This species was not detected in plasma from the same donors in the absence of visible light and RB exposure (Fig. 3A, lanes 8, 10, 12). This band was also not detected in plasma samples from donors with low CRP level (Fig. 3A, lanes 3, 5, 7), nor in other controls (Fig. 3A, lanes 2, 4, 6). Time course experiments carried out with plasma samples with high CRP levels, using the anti-CRP antibody, showed that increasing lengths of photolysis in the presence of RB/O_2 gave rise to a greater extent of protein crosslinking (Fig. 3B, lane 5 versus lanes 6, 8, 10), with a ~30-fold increase detected after 30 min, when compared to 0 min illumination (Fig. 3E). In accordance with the data obtained in the pre-oxidation experiments described above, pre-incubation of the plasma samples with NEM (1 mM) for 1 h before photooxidation markedly decreased the yield of protein crosslinks (Fig. 3B, lanes 7, 9, 11). In these experiments a further band was observed at ~100 kDa which also increased with increasing photolysis time and which was also recognized by the anti-CRP antibody: this is assigned to two CRP molecules crosslinked to a single HSA molecule (Fig. 3B, lanes 6, 8, 10). Neither of the CRP-HSA crosslinked species were observed in control samples where plasma was illuminated in the absence of RB, or when the plasma samples were incubated with RB without illumination (Fig. 3B, lanes 4 and 5).

In order to examine whether the crosslink between CRP and HSA is reducible, as might be expected for a disulfide species, studies were carried out using DTT (1 mM) and TCEP (1 mM) which are commonly used to reduce disulfide linkages. These compounds were added into plasma samples with high CRP levels that had been previously photooxidized (as described above) with the samples then further incubated for 1 h at 37 °C. Subsequent SDS-PAGE and immunoblotting analysis with either the anti-CRP or anti-HSA antibodies showed that the extent of crosslink formation was reduced significantly by treatment with either DTT or TCEP (Fig. 3, panels C, D, lanes 4–6). Densitometric analysis of these bands is presented in Fig. 3F.

To confirm the presence of reducible crosslinks between CRP and HSA in both the isolated protein and plasma samples, after incubation of photooxidized CRP with HSA or human plasma, the proteins were subjected to SDS-PAGE separation under both non-reducing and reducing

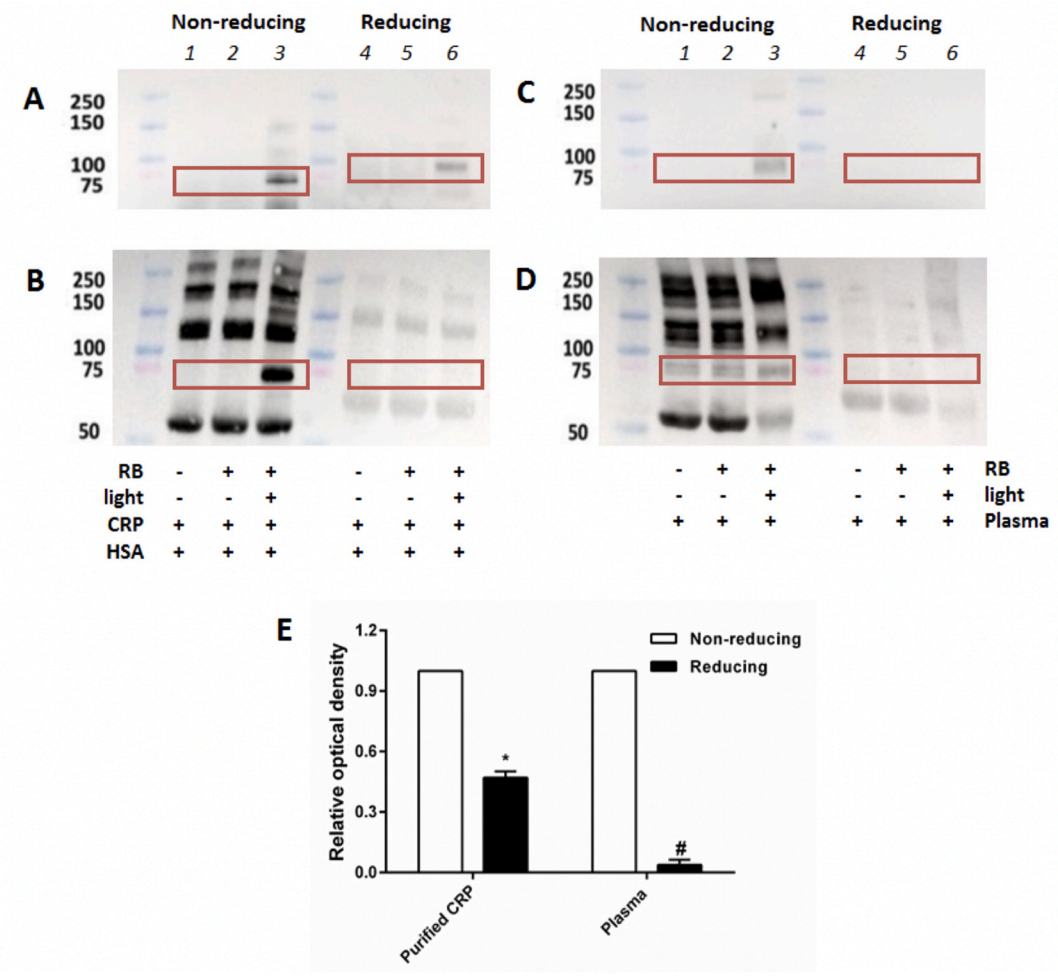

Fig. 4. Reversibility of pre-formed CRP-HSA crosslinks. CRP (5 μM in 10 mM phosphate buffer, pH 7.4) was subjected to RB-induced photolysis for 30 min and then incubated with HSA (5 μM in 10 mM phosphate buffer, pH 7.4) for 1 h, or plasma samples (donors with high CRP level) was exposed to RB-induced $^1O_2$ for 30 min. Subsequently the crosslinked samples were subjected to SDS-PAGE under non-reducing (panels A–D, lanes 1–3) or reducing condition (panels A–D, lanes 4–6). Panels A and B: Formation of CRP-HSA crosslinking between oxidized CRP and HSA, as detected using an anti-CRP antibody and an anti-HSA antibody, respectively. Panels C and D: Detection of CRP-HSA crosslinking in plasma samples (donors with high CRP level) after photolysis for 30 min, as detected by immunoblotting using an anti-CRP antibody and an anti-HSA antibody, respectively. Panel E: Optical density ($OD_{lane\ 3}$ vs. $OD_{lane\ 6}$) of crosslinked bands (~75k Da) from immunoblotting data in panels A and C. Statistical differences are indicated as follows: *P <0.05 vs. lane 3 (panel A), $^{\#}P < 0.05$ vs. lane 3 (panel C). Error bars represent SD of at least three independent experiments.

conditions before immunoblotting using either anti-CRP or anti-HSA antibodies. As shown in Fig. 4, panels A–D the crosslinked species were detected using both antibodies at a mass of ~75 kDa for the samples run under non-reducing conditions, but under reducing conditions these species were either markedly reduced in concentration or completely absent. These data are quantified in Fig. 4, panel E.

3.4. Detection of CRP-HSA crosslinks after exposure of plasma to different sources of $^1O_2$

In order to obtain further information on the mechanism of CRP-HSA crosslink formation, two alternative photosensitizers riboflavin (RF, 35 μM) and methylene blue (MB, 50 μM) were employed. Similar immunoblotting experiments were carried out to those outlined in sections 3.2 and 3.3. Thus, exposure of purified CRP to RF- or MB-induced photooxidation, and subsequent incubation with HSA showed clear formation of CRP-HSA crosslink when both anti-CRP or anti-HSA antibodies were employed (Fig. 5, panels A, B, E, F). The intensity of the new band at ~75 kDa increased in a time-dependent manner, with both sensitizers, with the CRP-HSA crosslink visible after 5 min illumination (Fig. 5, panels A, B, E and F, lanes 4–6), and a similar extent of increase in the yield of protein crosslinks after photolysis was determined for both sensitizers (Fig. 4, panels C and G).

The formation of species assigned to CRP-HSA crosslinks was also detected after exposure of plasma samples to both the RF- or MB-mediated photooxidation systems (Fig. 4, panels A, B, E and F, lanes 10–12). For both photooxidation systems, marked increases in the intensity of the band at ~75 kDa were detected using the anti-CRP antibody, and less significant changes with the anti-HSA antibody (Fig. 4, panels D and H). In the case of the anti-CRP antibody, these changes were statistically significant after 5 min photolysis, the shortest time point examined. The differences between the two antibodies is likely to be due to the sensitivity of these species in recognizing their respective antigens. Control samples illuminated in the absence of photosensitizers showed little, or no, immuno-reactivity at the corresponding positions on the membranes probed with the anti-CRP antibody, though weak bands were detected with the HSA antibody at a slightly higher mass (Fig. 4, panels A, B, E and F; lane 8). Similarly, little or no immunoreactivity was detected on the membranes at this mass, for samples incubated with the sensitizers in the absence of light (Fig. 4, panels A, B, E and F; lane 9).

3.5. Detection of CRP-HSA crosslinks after exposure of purified CRP/HSA systems and plasma to HOCl and ONOOH

The potential role of other oxidants in inducing similar crosslinks was examined using both the purified CRP/HSA (both 5 μM) and plasma (2 mg protein mL^{-1}, CRP level: 7.3–8.6 μg mL^{-1}) systems using both hypochlorous acid (HOCl) and peroxynitrous acid (ONOOH) as oxidants. These species are powerful oxidants formed at sites of inflammation by activated leukocytes (reviewed: [56,70]).

For isolated CRP, the protein was incubated with increasing concentrations of HOCl (5, 50, 500 and 1000 μM, corresponding to 1-, 10-, 100- and 200-fold molar excesses over the protein) for 1 h, with the pre-oxidized samples then incubated with HSA for an additional 1 h. Subsequent immunoblotting analysis (as described above) showed the formation of the putative CRP-HSA crosslink band at ~75 kDa, with HOCl concentrations of 500 μM or above, using both the anti-CRP (Fig. 6A, lanes 4, 5) and anti-HSA antibodies (Fig. 6B, lanes 4, 5), with the immunopositive bands more intense at higher oxidant concentration. With the anti-CRP antibody an additional weak band at ~50 kDa was also detected, probably from a CRP dimer species (Fig. 6A). Control incubations where buffer was added in place of HOCl, showed no immunoreactivity at the corresponding positions on the membranes (Fig. 6A, B, lane 1). For the plasma samples treated with HOCl at similar concentrations, immunoreactivity was also detected at ~75 kDa with

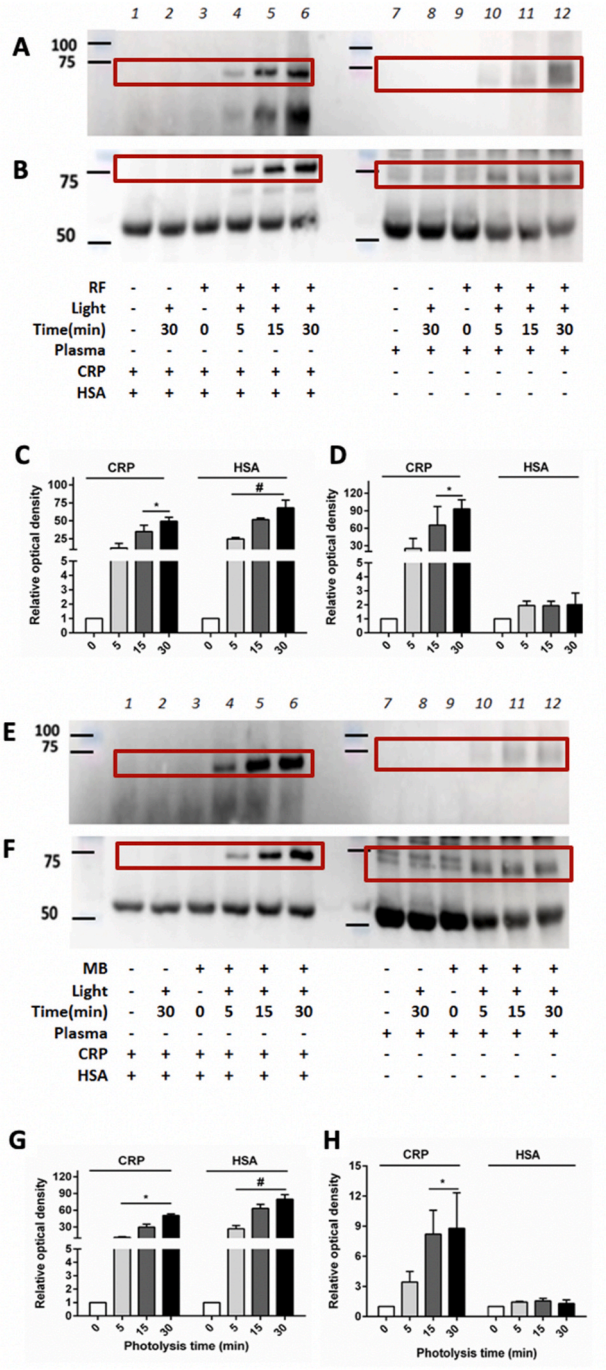

Fig. 5. Immunoblotting detection of CRP-HSA crosslinks after exposure of purified CRP or plasma to different sources of $^1O_2$. Panel A and B: Purified CRP (5 μM) reacted with riboflavin-induced $^1O_2$ with subsequent incubation with HSA for 1 h (lanes 1–6), or photo-oxidation of plasma samples containing high CRP levels (7.3–8.6 μg mL^{-1}, lanes 7–12) yielded CRP-HSA crosslinks, as detected by an anti-CRP antibody and an anti-HSA antibody, respectively. Panel C: Optical density ratio ($OD_{n\ min}/OD_{0\ min}$, n = 0, 5, 15 and 30 min) of CRP-HSA crosslinked bands from lanes 3–6 in panels A and B. Panel D: As panel C but for lanes 9–12 in panels A and B. Panels E and F: as panels A and B, but with photo-oxidation using methylene blue as the sensitizing dye. Panel G: Optical density ratio ($OD_{n\ min}/OD_{0\ min}$, n = 0 min, 5 min, 15 min and 30 min) of CRP-HSA crosslinked bands from lanes 3–6 in panels E and F. Panel H: as panel G, but data for lanes 9–12 in panels E and F. Statistical differences are indicated as follows: $^*P < 0.05$ vs. lane 3 or lane 9 (panels A and E), $^{\#}P < 0.05$ vs. lane 3 or lane 9 (panels B and F). Error bars represent SD of at least three independent experiments. (For interpretation of the references to color in this figure legend, the reader is referred to the Web version of this article.)

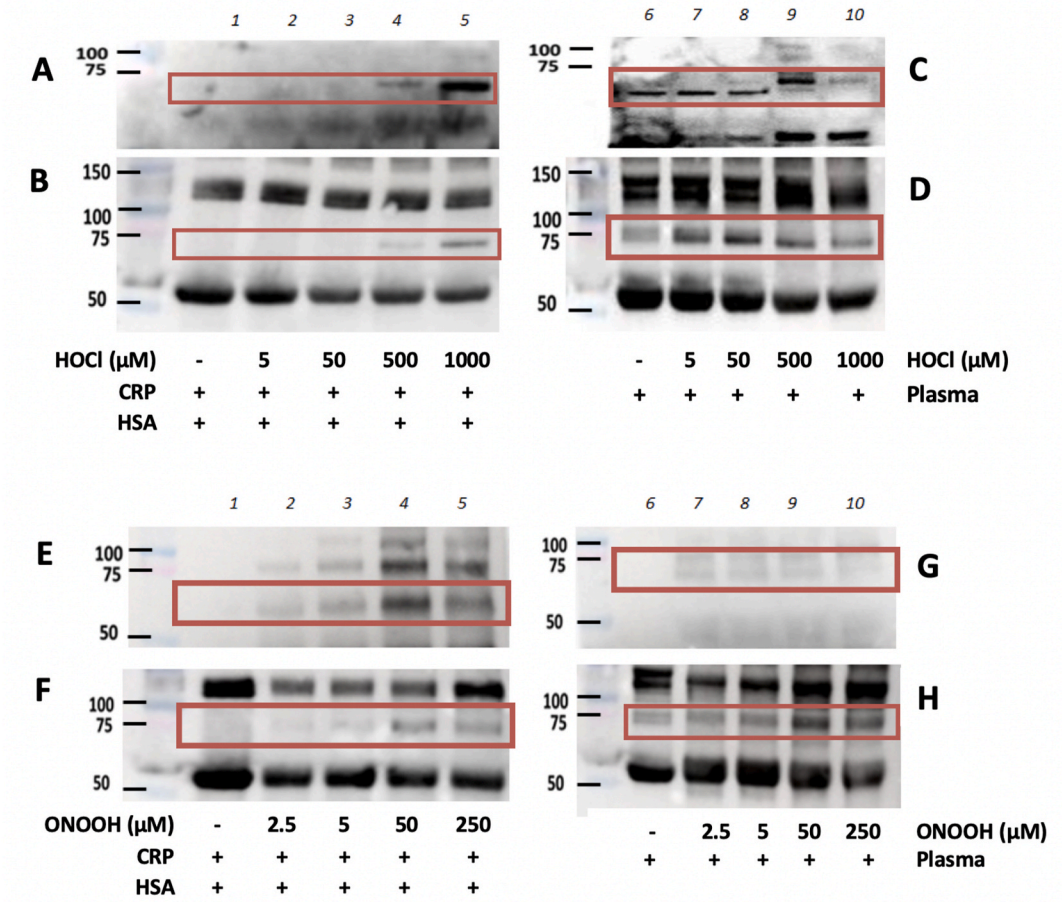

Fig. 6. Detection of CRP-HSA crosslinks by immunoblotting after exposure of purified CRP and plasma to HOCl and ONOOH. Panel A and B: Purified CRP (5 μM) was exposed to 1, 10, 100 and 200-fold molar excesses of HOCl (i.e. 5, 50, 500 or 1000 μM) and incubated for 1 h, before addition of HSA (5 μM) and incubation for 1 h. Samples were separated by SDS-PAGE and blotted onto PVDF membranes and developed using an anti-CRP antibody and an anti-HSA antibody, respectively. Panels C and D: Plasma samples (protein concentration: 2 mg mL^{-1}, CRP level: 7.3–8.6 μg mL^{-1}) were exposed to 5, 50, 500 or 1000 μM HOCl and incubated for 1 h, with subsequent immunoblotting and use of an anti-CRP antibody and an anti-HSA antibody, respectively. Panels E and F: Exposure of purified CRP (5 μM) to 0.5, 1, 10 or 50-fold molar excesses of ONOOH (2.5, 5, 50 or 250 μM) for 30 min, followed by reaction with HSA (5 μM) for 1 h. CRP-HSA crosslinks were detected by immunoblotting using an anti-CRP antibody and an anti-HSA antibody, respectively. Panels G and H: Detection of CRP-HSA crosslinks after exposure of plasma samples (protein concentration: 2 mg mL^{-1}, CRP level: 7.3–8.6 μg mL^{-1}) to 2.5, 5, 50 or 250 μM concentrations of ONOOH for 30 min, with detection of CRP-HSA crosslinks by immunoblotting using an anti-CRP antibody and an anti-HSA antibody, respectively.

both antibodies (Fig. 6, panels C and D), but the pixel intensity was decreased at the highest concentrations of HOCl used (1000 μM) possibly due to over-oxidation of the samples (Fig. 6, panels C and D, lane 10). At these high oxidant excesses, a significant loss of the parent HSA band was also detected (Fig. 6, panel D, lanes 9 and 10).

ONOOH treatment of purified CRP (5 μM) followed by reaction with HSA (5 μM), in a similar manner to that described above, also resulted in the detection of immunoreactivity at the molecular mass of the putative CRP-HSA crosslink, with the intensity of this increasing in an oxidant dose-dependent manner, as detected using both the anti-CRP and anti-HSA antibodies, though the intensity decreased again at the highest ONOOH concentration (Fig. 6, panels E and F, lanes 2–5). Similar bands at ~75 kDa were also detected in the oxidized plasma samples treated with identical ONOOH concentrations, though the intensity of the proposed crosslink band decreased with the highest concentration of ONOOH (Fig. 6, panels G and H, lanes 7–10). Little or no immunoreactivity was detected at a molecular mass of ~75 kDa for controls where buffer was added in place of ONOOH (Fig. 6, panels G and H, lane 6).

3.6. LC-MS/MS analysis of crosslink and parent protein bands

Gel bands, from photooxidation experiments with RB/visible light and the isolated protein followed by incubation with HSA or plasma (low CRP levels), corresponding to native CRP, native HSA, and CRP-HSA crosslinks, were cut from multiple representative gels. These were then subjected to dual enzyme (trypsin followed by Glu-C) in-gel digestion followed by nanoLC-MS/MS analysis as described in the Materials and methods. The species identified (number of peptides and sequences) from each sample, and the corresponding proteins to which these are assigned, are summarized in Table 1. The LC-MS/MS analysis of the parent protein bands showed, as expected, large numbers of peptides consistent with the presence of native CRP (16 peptides, covering 61.7% of the protein sequence) and native HSA (52 peptides, covering 74.5 % of the protein sequence). A small number of these peptides contained missed cleavages and, for HSA, the presence of five peptides with methionine (Met) residues present as the corresponding sulfoxide (i.e. as m/z +16 species, Table 1). Analysis of the band assigned to the CRP-HSA crosslink from the isolated protein experiments (i.e. pre-oxidized isolated CRP subsequently incubated with HSA) showed the presence of 6 peptides from CRP (24.8% sequence coverage) and 42 peptides from HSA (61.2 % sequence coverage) (Table 1). Selected peptides arising from both CRP and HSA arising from the crosslinked species are presented in Fig. 7. Similarly, the CRP-HSA crosslink detected from the experiments in which CRP was subjected to photooxidation and then incubation with plasma containing low CRP levels, showed the presence of 6 CRP peptides (25.7% sequence

Table 1
Peptides (and identified proteins) from sequential in-gel digestion with trypsin and GluC followed by LC-MS/MS analysis.

Protein ID	Accession number[a]	Peptide sequence	m/z[b]	Charge state	Mass error (ppm) [c]	Detected sample[d]		
						CON protein band	CRP-HSA band	CRP-Plasma band
C reactive protein (CRP)	P02741	AFTVC*LHFYTE	694.32	2	0.15	×		
		AFTVC*LHFYTELSSTR	644.65	3	0.10	×		
		AFVFPK	354.71	2	0.86	×	×	×
		ALKYEVQGEVFTK	504.61	3	1.74	×		
		APLTKPLK	434.29	2	1.10	×	×	
		ESDTSYVSLK	564.78	2	0.68	×	×	×
		FWVDGKPR	335.52	3	0.96	×		
		GYSIFSYATK	568.79	2	0.40	×	×	×
		DIGYSFTVGGSEILFEVPE	1030.00	2	0.78	×		
		ILIFWSK	453.78	2	0.71	×	×	×
		RQDNEILIFWSK	774.91	2	0.68	×		×
		SASGIVEFWVDGKPR	549.95	3	0.20	×		
		VFTKPQLWP	558.32	2	0.03	×		
		VTVAPVHIC*TSWE	749.87	2	0.36	×		
		YEVQGEVFTK	600.30	2	0.40	×	×	
		YEVQGEVFTKPQLWP	910.96	2	0.02	×		×
Human Serum albumin (HSA)	P02768	AAC*LLPK	386.72	2	0.44	×	×	
		AAFTEC*C*QAADK	686.29	2	0.02	×	×	×
		AEFAEVSK	440.72	2	0.58	×	×	×
		ALVLIAFAQYLQQC*PFEDHVK	830.77	3	0.67	×	×	×
		AWAVAR	337.19	2	0.59	×		
		AVM(ox)DDFAAFVEK	679.82	2	0.87	×	×	×
		C*C*AAADPHEC*YAK	518.20	3	0.53	×	×	
		C*C*EKPLLEK	588.79	2	0.57	×		
		C*C*TESLVNR	569.75	2	2.78	×	×	×
		C*FLQHK	416.71	2	2.11	×		
		DDNPNLPR	470.73	2	0.38	×	×	×
		DLGEENFK	476.22	2	0.79	×	×	×
		DYLSVVLNQLC*VLHEK	965.51	2	0.94	×		
		DVFLGMFLYEYAR	812.39	2	1.06	×		
		DVFLGM(ox)FLYEYAR	820.39	2	0.58	×	×	×
		EFNAETFTFHADIC*TLSEK	1130.52	2	0.27	×	×	×
		ETC*FAEEGK	535.73	2	0.61	×	×	
		ETYGEM(ox)ADC*C*AK	725.77	2	0.55	×	×	×
		FKDLGEENFK	613.81	2	0.12	×	×	×
		FKPLVEEPQNLIK	777.95	2	0.49	×		
		FQNALLVR	480.78	2	0.75	×	×	×
		HPDYSVVLLLR	656.37	2	0.20	×	×	×
		HPYFYAPELLFFAK	581.64	3	0.49	×		
		HPYFYAPE	512.23	2	0.21		×	×
		KLVAASQAALGL	571.35	2	1.48	×	×	×
		KQTALVELVK	376.90	3	1.45	×	×	
		KVPQVSTPTLVEVSR	820.47	2	0.29	×	×	×
		KYLYEIAR	352.53	3	0.57	×	×	×
		LC*TVATLR	467.26	2	2.46	×	×	×
		LLFFAK	369.73	2	0.58	×	×	×
		LDELRDEGK	537.78	2	0.47	×	×	×
		LVAASQAALGL	507.30	2	0.12	×	×	×
		LVNEVTEFAK	575.31	2	0.43	×	×	×
		LVTDLTK	395.24	2	0.46	×	×	×
		LVRPEVDVM(ox)C*TAFHDNE	683.31	3	0.80	×		
		NEC*FLQHKDDNPNLPR	499.99	4	0.56	×	×	×
		PLVEEPQNLIK	640.37	2	0.73	×	×	
		NYAEAK	695.34	1	1.68	×		×
		QNC*ELFEQLGEYK	829.38	2	0.03	×	×	×
		QTALVELVK	500.81	2	0.14	×	×	×
		RPC*FSALEVDE	661.81	2	0.94	×		
		RHPDYSVVLLLR	489.95	3	0.22	×	×	×
		RHPYFYAPE	590.28	2	0.26	×	×	×
		RPC*FSALEVDETYVPK	637.65	3	0.24	×	×	×
		SLHTLFGDK	339.85	3	0.87	×	×	×
		TC*VADESAENC*DK	749.79	2	1.18	×	×	×
		TPVSDR	337.68	2	0.63	×	×	×
		TYETTLEK	492.75	2	0.60	×	×	×
		VDVM(ox) C*TAFHDNEETFLKK	550.76	4	1.11	×		
		VHTEC*C*HGDLLEC*ADDR	522.47	4	1.50	×	×	×
		VPQVSTPTLVEVSR	756.43	2	1.03	×	×	×
		YIC*ENQDSISSK	722.33	2	0.27	×	×	×
		YLYEIAR	464.25	2	0.90	×	×	×

Control proteins (CRP and HSA) and gel bands from the proposed crosslink at ~75 kDa (CRP-HSA), generated from photooxidation of CRP with RB/visible light and subsequent incubation with HSA, or plasma containing a low level of CRP, were cut from multiple representative gels and subsequently analyzed by in-gel digestion coupled with MS spectrometry. Proteins were obtained from 3 separate batches.

[a] Accession numbers correspond to the UniProt database.

[b] Observed mass-to-charge ratio (*m/z*).

[c] Mass errors were determined using Maxquant.

[d] Protein gel bands that contain the detected peptides. Asterisks (*) indicates alkylation of the noted Cys residue with a mass shift of +57 Da. M(ox) refers to methionine residues detected as oxidized (sulfoxide) species (+16 Da). Analysis of peptide mass mapping data was performed using GPMAW 9.5 software with manual validation.

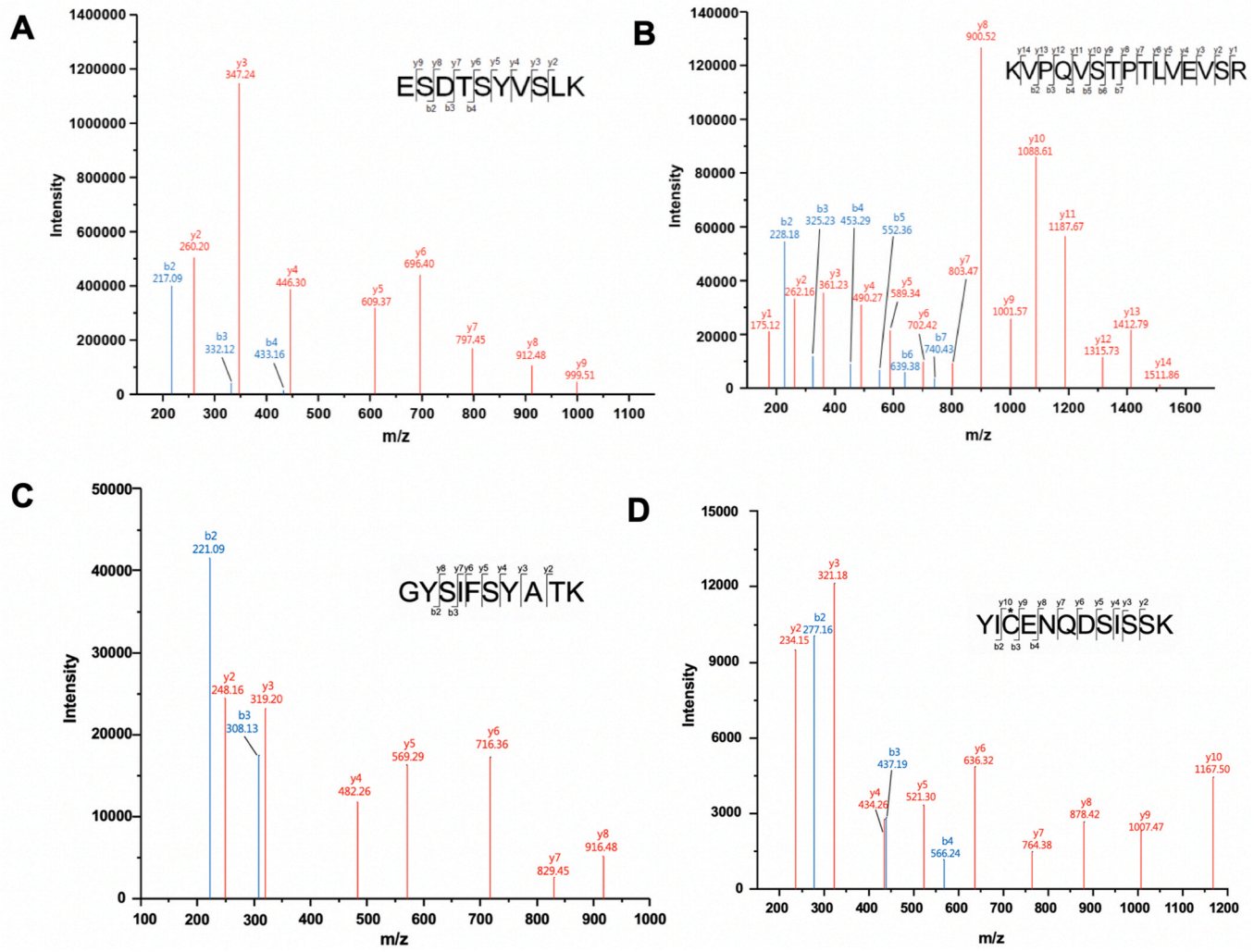

Fig. 7. MS/MS fragment ion spectra of CRP and HSA from CRP-HSA crosslinked gel bands. Panel A: Representative MS/MS spectrum of peptide ESDTSYVSLK (*m/z*: 564.78; charge state: +2; mass error: 0.68 ppm) from CRP detected in CRP-HSA crosslinked gel band (band at ~ 75 kDa). Panel B: Representative MS/MS spectrum of peptide KVPQVSTPTLVEVSR (*m/z*: 820.47; charge state: 2+; mass error: 0.29 ppm) from HSA detected in CRP-HSA crosslinked gel band (band at ~ 75 kDa). Panel C: Representative MS/MS spectrum of peptide GYSIFSYATK (*m/z*: 568.79; charge state: 2+; mass error: 0.40 ppm) from CRP detected in CRP-HSA crosslinked gel band after reaction of photo-oxidized CRP and plasma (band at ~ 75 kDa). Panel D: Representative MS/MS spectrum of peptide YIC*ENQDSISSK (where * indicates carbamidomethylation of the Cys residues: + 57 Da; *m/z*: 722.33; charge state: 2+; mass error: 0.27 ppm) detected in CRP-plasma crosslinked gel band after reaction of photo-oxidized CRP and plasma (band at ~ 75 kDa). Red fragments correspond to the y ions, and blue fragments correspond to the b ions. (For interpretation of the references to color in this figure legend, the reader is referred to the Web version of this article.)

coverage) and 38 HSA peptides (57.1%) (Table 1). As with the native protein samples, a small number of these peptides arise from missed cleavages, and three peptides were detected with Met present as the corresponding sulfoxide. The numbers of peptides detected from the crosslinked species were lower than for the parent proteins, likely reflecting the lower concentrations of the crosslinked species compared to the parent species, and also (probably) a decreased efficiency of digestion of the crosslinked species in the gel matrix. Despite the lower numbers of peptides detected from the crosslinked species, the detection of a wide range of distinctive peptides from *both* proteins in these bands strongly supports the conclusion that these bands contain both CRP and HSA and hence (one or more) crosslinked species containing these two proteins.

Further data on the nature of the crosslinked species formed between CRP and HSA was obtained from in solution digestion of the isolated protein samples and subsequent LC-MS/MS analysis. Thus, samples of CRP were photooxidized using the RB/O_2 system for 30 min, and then incubated with HSA (as described above). Subsequent LC-MS/MS

analysis showed the presence of ions consistent with the presence of a crosslinked peptide containing a disulfide cross-link with sequence (AFTVCLHFYTELSSTR) (ALVLIAFAQYLQQCPFEDHVK) with the first peptide (α peptide) containing Cys36 from CRP, and the second peptide (β peptide) containing Cys34 from HSA. Fig. 8, panel A, shows a representative MS/MS spectrum obtained from this crosslinked peptide with precursor ion *m/z* 718.3690 (mass error 13.9 ppm) in the +6 charge state. The fragmentation ions obtained from this peptide include multiple species retaining the crosslink, confirming the site of the linkage and the residues involved (Fig. 8A). Fig. 8B shows the extracted ion chromatogram for the precursor ion matching the crosslink peptide; this ion was not detected in control samples where non-oxidized CRP was incubated with HSA (black line), in samples containing all components of the reaction system, but with no illumination (blue line, 0 min), nor in samples where the crosslinked proteins were subsequently incubated with DTT and IAM to reduce and alkylate the disulfide linkage after the trypsin digestion. The LC-MS/MS spectrum of the reduced and alkylated peptide arising from this last treatment is presented in Supplementary Fig. 1. The extracted ion chromatogram from the (reduced and alkylated) parent peptide from HSA (ALVLIAFAQYLQQC*PFEDHVK, with the Cys residue carbamidomethylated) showed the inverse behavior with the highest intensity of the precursor ion from this peptide (*m/z* 623.3267, +4 charge state, mass error 8.5 ppm) detected in the samples where the CRP was subject to photooxidation, incubated with HSA, then subjected to treatment with DTT and IAM (Fig. 8C). Quantification of the ion intensities of both the crosslinked and parent HSA peptides for these various conditions, are given in Fig. 8, panels D and E. These data confirm the presence of a disulfide crosslink between the Cys36 residue of CRP and Cys34 of HSA, which is formed only after oxidation of CRP, with this new oxidation-dependent crosslink being readily reduced by treatment with DTT.

4. Discussion

Oxidative stress is associated with a large number of pathologies, and particularly those associated with acute or chronic inflammation, such as cardiovascular diseases (including atherosclerosis), diabetes, rheumatoid arthritis, fibrotic diseases and multiple neurodegenerative diseases (reviewed [20]). Both acute and chronic inflammation are associated with increased formation of oxidants, such as HOCl and ONOOH, which are generated via enzymatic activity (myeloperoxidase in the case of HOCl, and the combined actions of nitric oxide synthase and NADPH oxidases in the case of ONOOH). Oxidants are also formed as a result of exposure to multiple external stimuli such as various forms of radiation (high energy, UV and visible light in the presence of a sensitizer), metal ions, pollutants, drugs and solvents [20]. Excited state species, such as $^1O_2$, are generated by multiple endogenous processes and also exogenous stimulants, including peroxyl radical termination reactions (e.g. of lipid peroxyl radicals generated during lipid peroxidation), reaction of H_2O_2 with HOCl, metal ion- and heme-protein mediated redox processes, and from Type 2 photochemical reactions, where energy from an initial excited state species is transferred to O_2 [20,67,71,72].

Proteins are especially vulnerable to oxidative damage as a result of their high concentrations *in vivo* and rapid rates of reaction with a number of oxidants, leading to the formation of oxidation products that can modulate their composition, structure and function [5,73]. Proteins are abundant in extracellular compartments (e.g. 1–3 mM in plasma), and therefore plasma proteins are likely to be major targets [5,74]. Rate constants have been reported for the reactions of HOCl, ONOOH and $^1O_2$ with amino acid residues (and models of these) present in proteins, and for most oxidants the sulfur-containing amino acids (Cys, Met and cystine) are the most rapidly modified [75–79]. Many extracellular proteins contain relatively low abundances of Cys, and modest levels of Met, whereas cystine disulfide bonds are relatively abundant, suggesting that disulfide bonds may be particularly important oxidant targets outside cells (e.g. in extracellular fluids, plasma and in the extracellular matrix).

In humans, CRP is primarily synthesized by liver hepatocytes and secreted into plasma. The level of CRP in peripheral blood is used clinically [80,81] as a short-lived marker of systemic inflammation (plasma half-life ~ 19 h [51], with this being invariant with health and disease [82]). CRP levels vary from <50 μg L^{-1} to more than 500 mg L^{-1} (i.e. ~ 22 μM) following an acute stimulus [80]. This increased concentration suggests that CRP may be a significant target for oxidants under conditions of inflammation, and that damage to this protein may be both a marker of oxidative stress, and also a potential mediator of ongoing inflammation.

In the current study, both purified monomeric CRP (mCRP), and plasma containing high CRP levels, were exposed to RB-induced photooxidation which generates high yields of $^1O_2$ (quantum yield, φ^{RB}, of 0.7–0.8 [83]). This resulted in time-dependent loss of mCRP (Fig. 1) for both the purified system (by immunoblotting) and the oxidized plasma samples (by ELISA). Concomitant formation of a band assigned to a CRP dimer was detected when the isolated CRP system was examined with higher protein concentrations (Fig. 2A). Oxidation was also detected with HOCl and ONOOH, consistent with a previous report [55]. These data establish that CRP is readily modified by multiple oxidants, both in isolation and also in more complex systems such as plasma.

Our previous studies, and other research on model systems, have provided evidence for the formation of zwitterion peroxides [RS-S^+(-OO^-)R] on reaction of both low-molecular-mass and protein disulfides, with $^1O_2$, and thiosulfinates [RS-S(=O)R] with two electron oxidants [40–42,44–48]. These species have modest lifetimes (several hours [42]), but undergo subsequent rapid reaction with other thiols to give thiolated proteins in which the original disulfide bond is cleaved, and a new disulfide generated between the added thiol and one of the Cys residues of the original disulfide. This process has been termed 'oxidant-mediated thiol-disulfide exchange' [42]. Whilst initial studies examined reaction with low-molecular mass thiols (e.g. GSH, *N*-acetyl cysteine [40–42], reaction can also occur with a thiol group present on a second protein (e.g. GAPDH) with this yielding a new protein-protein crosslink [43]. The current study extends this work to show that CRP undergoes this type of reaction with HSA, both in isolated systems and also in fresh human plasma, with reaction occurring between Cys34 on HSA and one of the Cys residues (Cys36) of the former disulfide of CRP. Thus, a new species is observed at an apparent mass of ~75 kDa when the pre-oxidized CRP was subsequently incubated with HSA. The formation of this species was inhibited by pre-treatment of the HSA with NEM to block the free thiol (Figs. 2, 3). This band was recognized by both anti-CRP and anti-HSA antibodies consistent with the presence of both proteins. The apparent molecular mass of this species (~75 kDa) is lower than that expected from the combined mass of the two parent proteins (23 kDa and 66.5 kDa respectively). The reason for this anomalous apparent mass (commonly called 'gel shifting') is not completely resolved, but is a common feature of gels run under non-reducing conditions, and is widely observed. It has been proposed to result from altered detergent/surfactant binding, or the pI of the protein [84,85], though it may also be related to altered migration of dimeric species. The LC-MS/MS analyses carried out on the excised gel bands from this species, provide very strong evidence for the presence of both CRP and HSA in this band, and supports its assignment to a novel CRP-HSA dimer.

The extent of formation of this CRP-HSA species is dependent on the extent of initial CRP oxidation, and hence (presumably) the yield of zwitterion peroxide or thiosulfinate, though these are very difficult to quantify experimentally due to their instability, and lack of authentic standards. Direct photooxidation in the absence of the sensitizers did not generate these species, consistent with a key role for $^1O_2$ in these reactions (see also [44]). Similar crosslinks were detected with all three photosensitizers, suggesting common intermediate species, believed to

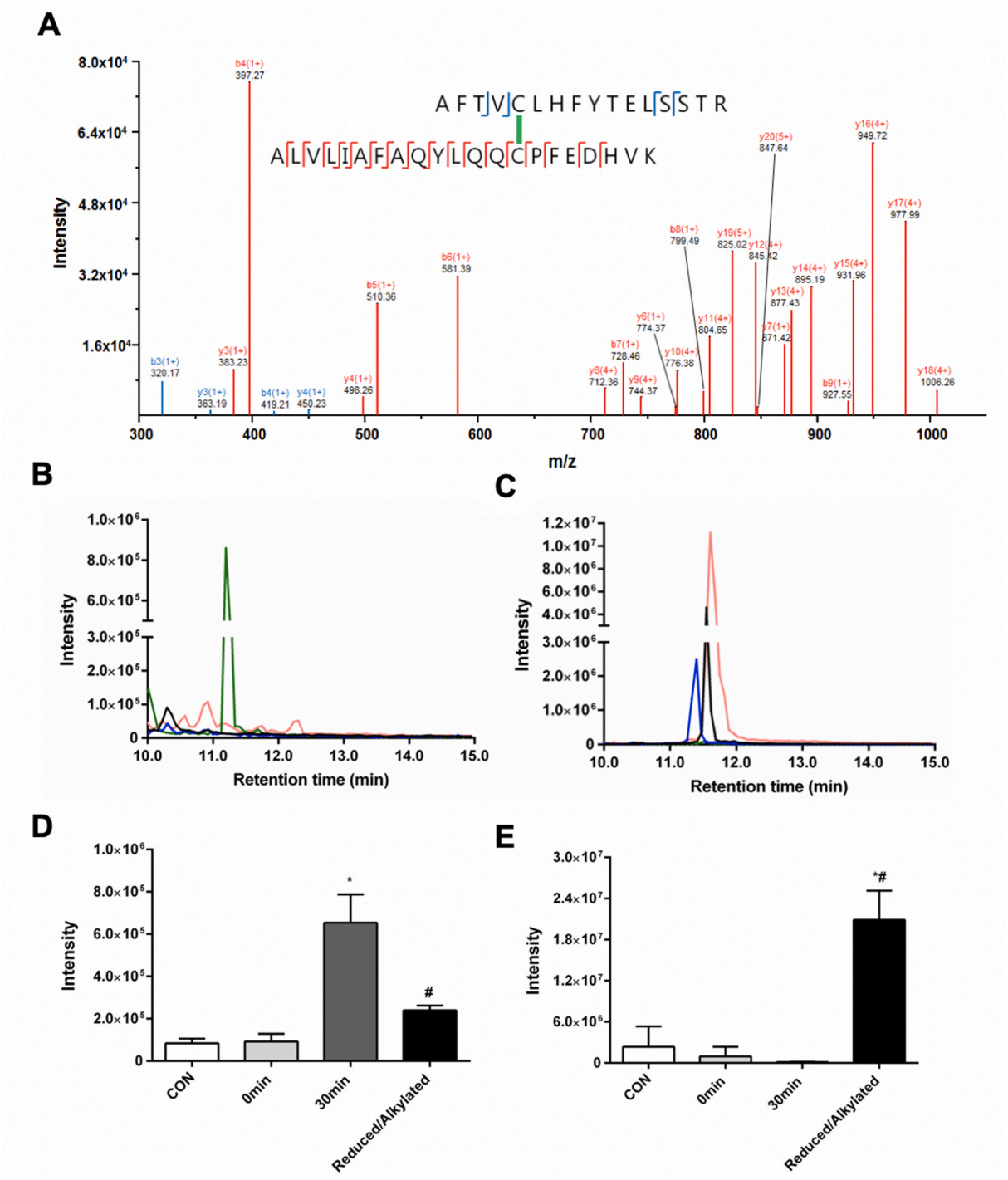

Fig. 8. LC-MS/MS characterization of the novel new inter-protein disulfide formed between Cys36 of CRP and Cys34 of HSA. Panel A: Assignment of MS/MS spectrum of a +6 charge state precursor ion (*m/z* 718.3690) matching the crosslinked peptide (AFTVCLHFYTELSSTR) (ALVLIAFAQYLQQCPFEDHVK) with the first shorter peptide (α peptide) containing Cys36 from CRP, and the second longer peptide (β peptide) containing Cys34 from HSA. Blue y and b fragments correspond to the α peptide, while red y and b fragments correspond to the β peptide. Panel B: Extracted ion chromatogram (EIC) of the precursor ion with *m/z* 718.3690 (+6 charge state) for the crosslinked peptide. Panel C: Extracted ion chromatogram of the precursor ion with *m/z* 623.3267 (+4 charge state) for the linear peptide ALVLIAFAQYLQQ**C***PFEDHVK (where * indicates carbamidomethylation of the Cys residue, +57 Da). Black line: control (CON) where purified CRP was incubated with purified HSA for 30 min and subsequently subjected to trypsin digestion; blue line: purified CRP illuminated for 0 min in the presence of RB, followed by incubation with purified HSA for 1 h and trypsin digestion; green line: purified CRP exposed to RB-induced $^1O_2$-mediated photooxidation for 30 min, followed by incubation with purified HSA for 1 h and trypsin digestion; red line: purified CRP exposed to RB-induced $^1O_2$-mediated photooxidation for 30 min, followed by incubation with purified HSA for 1 h and overnight digestion with trypsin (i.e. as green line) but with the samples subsequently treated with DTT (40 mM in 100 mM ammonium bicarbonate, pH 8.0) and IAM (100 mM in 100 mM ammonium bicarbonate, pH 8.0), and incubated for 45 min and 60 min, respectively. Panels D and E: total ion intensity from the EIC of the precursors with *m/z* 718.3690 (crosslinked peptide, panel B) and 623.3267 (reduced and alkylated HSA peptide, panel C), respectively. The statistical differences are indicated as follows: *$P < 0.05$ versus CON (panels D and E); $^{\#}P < 0.05$ versus 30 min photo-oxidized sample (panels D and E). Quantitative data are presented as mean ± SD from three independent experiments. (For interpretation of the references to color in this figure legend, the reader is referred to the Web version of this article.)

be $^1O_2$ and a zwitterion peroxide formed from the Cys 36-Cys 97 disulfide bond of CRP. The (solid state) protein structure of CRP (Fig. 9) indicates that the disulfide bond in CRP is buried within the protein structure, suggesting that initial oxidation at this site, to give the (more hydrophilic and dipolar) peroxide may result in structural changes and partial unfolding. This would facilitate subsequent reaction of the zwitterion peroxide with the Cys34 residue of HSA; the latter is likely to react via the ionized form, RS^-, which is a better nucleophile. Initial oxidation of the (apparently buried) CRP disulfide bond is likely to be facilitated by the small neutral nature of $^1O_2$, which allows diffusion into proteins. Alternatively, oxidation may occur via transient unfolding of the CRP structure in solution (as observed in previous studies with beta-2-microglobulin and GAPDH [43]), where the single disulfide bond appears to be buried in the crystal structure, but hydrogen-deuterium exchange mass spectroscopy indicates the presence of unfolded states in solution [86,87].

Analogous species were detected with the biologically-relevant two-electron oxidants, HOCl and ONOOH, indicating that this may be a general mechanism of crosslink formation. Both these oxidants react rapidly with disulfides, and hence are kinetically-favorable reactions [40,88]. With these oxidants, the reactive intermediate formed from the disulfide may be a thiosulfinate (cf. previous studies [41,42]), though the products arising from subsequent reaction are similar. As with $^1O_2$, initial reaction at the CRP disulfide bond is likely to occur via the neutral forms of these oxidants (i.e. HOCl and ONOOH, and not $^-$OCl or $ONOO^-$) [70,75]. Formation of the thiosulfinate is likely to result in (at least partial) unfolding of the protein structure as this is a more polar and bulky species.

The new inter-protein linkage can be readily reduced by the reductants DTT and TCEP, which have been used extensively to reduce disulfide bonds, though they are not exclusive for these species (Fig. 3). A similar loss of the crosslink was detected with samples separated on gels run under reducing, rather than non-reducing, conditions (Fig. 4). Although other protein crosslinks involving Tyr, Trp, His, Lys, Arg, Met and dehydroalanine, have been detected after exposure of proteins to oxidants (e.g. Refs. [89–96]), these other crosslinks are not (or are poorly) removed by these reducing reagents, or by use of reducing gel conditions, as they contain strong carbon-carbon or carbon-heteroatom bonds.

This novel CRP-HSA dimer was also detected on oxidation of diluted plasma samples from multiple human donors that contain high, but not low, levels of CRP (Fig. 3). The different behavior of the plasma samples containing high-versus low- CRP levels suggests that there is (as expected) competition between the different proteins (and also other species) present in plasma for the oxidants, and that significant levels of modification of CRP only occur when the levels of this protein are elevated. Whilst the crosslink yield increased with longer photooxidation times for the sensitizer systems, the intensity of the crosslink band decreased with the highest concentrations of HOCl and ONOOH examined (Fig. 6). This may be due to competitive reaction of these oxidants with the Cys34 residue of HSA (which is rapid [76,97,98]), with this resulting in Cys34 depletion and therefore more limited reaction with oxidized CRP.

The precise location of the cross-link has been determined by LC-MS/MS analysis of digested protein samples (at least in the case of the RB/O_2 oxidation system) with a peptide detected involving a crosslink between Cys36 of CRP and Cys34 of HSA. Whilst the involvement of Cys34 of HSA is unsurprising, as it is the only free Cys residue on the latter protein, it is perhaps surprising that no evidence was obtained for a cross-link between HSA-Cys34 and the Cys97 residue of CRP, though detection of this residue in a single peptide proved problematic with trypsin digestion, and hence the formation of adducts at this residue

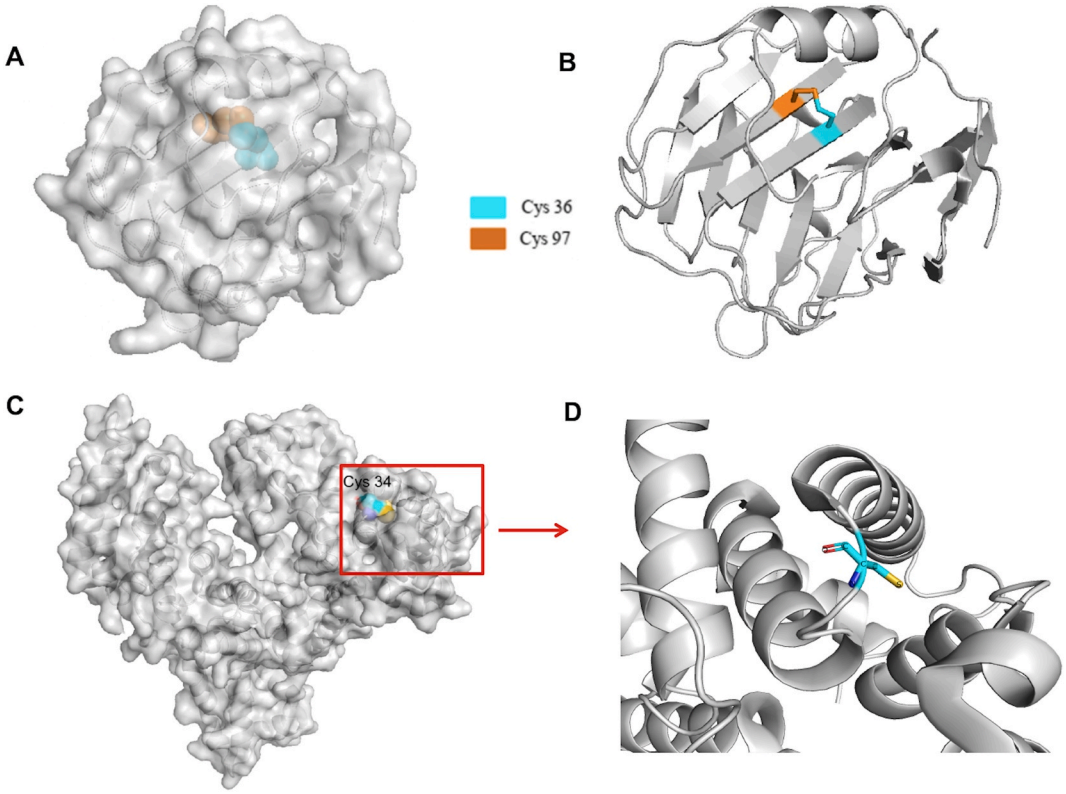

Fig. 9. Rendering of the structures of CRP (panels A and B) and HSA (panels C and D), showing the environment of the disulfide bond in CRP, and the Cys34 residue in HSA. Panels A (van der Waals spheres) and B (ribbon structure) generated from the crystal structure data of subunit A of pentameric CRP (PDB ID: 1B09), showing the internal intra-molecular disulfide Cys36 - Cys97, as indicated by the weak coloration of the residues in panel A. Panels C and D: environment of the single free Cys residue, Cys34, in HSA (PDB ID: 1N5U). The surface-accessible nature of Cys34 is indicated by the bright coloration.

cannot be completely discounted. Thus, there appears to be a selectivity for reaction with the Cys36 residue of the oxidized Cys36-Cys97 CRP disulfide bond. Whether this is related to the initial site of $^1O_2$ oxidation, the nature of (the possible) protein unfolding, or steric/electronic interactions between the two proteins that favor reaction at the Cys36 end of the CRP disulfide bond remains to be established. Further studies with a larger number of plasma samples with a wide range of CRP levels, and (semi-) quantification of the crosslink yield, may permit a 'cut-off' concentration of CRP for crosslink formation to be determined. Such studies would however need a considerable number of samples, due to the variations in plasma between subjects.

Consistent with our proposed mechanism, pretreatment of the plasma samples with the thiol-blocking reagent NEM significantly inhibited the intensity of the proposed CRP-HSA crosslink species (Figs. 2, 3), supporting the role of the Cys34 residue on HSA in the generation of these species. Whilst this has not been investigated as yet, it is possible that similar reactions occur with other thiols present on other plasma proteins (although these are present at much lower concentrations), and also with low-molecular-mass thiols present in plasma (e.g. cysteine, cysteinylglycine, glutathione, homocysteine, and γ-glutamylcysteine, which are present at ~12–20 μM in total [99]). Analogous reactions may also occur with other plasma proteins (e.g. immunoglobulins) that contain disulfide bonds, and this would appear to be worthy of further study in order to determine the generality of the reactions described here. Thus, the chemistry outlined here may be a common mechanism for the formation of reducible protein-protein crosslinks, including with proteins that do not contain initial free Cys residues.

HSA has been reported to have multiple biological activities including weak enzymatic activity involving a number of residues including Tyr, His, Trp and Lys residues (see, e.g. Ref. [100]). In addition, oxidation of Cys34, and subsequent thiolation (e.g. involving homocysteine or GSH), or cyclization with the adjacent Gln to form a sulfinamide, has been shown to alter the capacity of HSA to bind ligands, and has also been proposed as a biomarker of oxidative stress [38,101,102]. Thus, the reaction of this residue on HSA with oxidized CRP, as described here, has the potential to not only affect the biological activity of HSA, but also act as a (long-lived) marker of oxidant exposure.

Declaration of competing interest

The authors declare no conflicts of interest with regard to the data presented.

Acknowledgements

The authors are grateful for financial support from the Novo Nordisk Foundation (Laureate grants: NNF13OC0004294 and NNF20SA0064214 to MJD), the China Scholarships Council (PhD scholarship to SJ: 201708340066), a WHRI International Fellowship (to LC) co-funded by the People Programme (Marie Curie Actions) of the European Union's Seventh Framework Programme (FP7/2007–2013) under REA grant agreement nº 608765, and an infrastructure grant from the Carlsberg Foundation (CF19-0451 to PH).

Appendix A. Supplementary data

Supplementary data to this article can be found online at https://doi.org/10.1016/j.redox.2021.101925.

References

[1] P.J. Hogg, Disulfide bonds as switches for protein function, Trends Biochem. Sci. 28 (2003) 210–214.
[2] C.S. Sevier, C.A. Kaiser, Formation and transfer of disulphide bonds in living cells, Nat. Rev. Mol. Cell Biol. 3 (2002) 836–847.
[3] L.W. Ruddock, T.R. Hirst, R.B. Freedman, pH-dependence of the dithiol-oxidizing activity of DsbA (a periplasmic protein thiol:Disulphide oxidoreductase) and protein disulphide-isomerase: studies with a novel simple peptide substrate, Biochem. J. 315 (1996) 1001–1005.
[4] E. Gross, D.B. Kastner, C.A. Kaiser, D. Fass, Structure of Ero1p, source of disulfide bonds for oxidative protein folding in the cell, Cell 117 (2004) 601–610.
[5] M.J. Davies, Protein oxidation and peroxidation, Biochem. J. 473 (2016) 805–825.
[6] C. Klomsiri, P.A. Karplus, L.B. Poole, Cysteine-based redox switches in enzymes, Antioxidants Redox Signal. 14 (2011) 1065–1077.
[7] L.B. Poole, The basics of thiols and cysteines in redox biology and chemistry, Free Radic. Biol. Med. 80 (2015) 148–157.
[8] J. Yang, K.S. Carroll, D.C. Liebler, The expanding landscape of the thiol redox proteome, Mol. Cell. Proteomics 15 (2016) 1–11.
[9] P. Nagy, Kinetics and mechanisms of thiol-disulfide exchange covering direct substitution and thiol oxidation-mediated pathways, Antioxidants Redox Signal. 18 (2013) 1623–1641.
[10] D. Fass, C. Thorpe, Chemistry and enzymology of disulfide cross-linking in proteins, Chem. Rev. 118 (2018) 1169–1198.
[11] T.N. Vinther, T.B. Kjeldsen, K.J. Jensen, F. Hubalek, The road to the first, fully active and more stable human insulin variant with an additional disulfide bond, J. Pept. Sci. 21 (2015) 797–806.
[12] T.N. Vinther, M. Norrman, U. Ribel, K. Huus, M. Schlein, D.B. Steensgaard, T. A. Pedersen, I. Pettersson, S. Ludvigsen, T. Kjeldsen, K.J. Jensen, F. Hubalek, Insulin analog with additional disulfide bond has increased stability and preserved activity, Protein Sci. 22 (2013) 296–305.
[13] Y.W. Lin, Structure and function of heme proteins regulated by diverse post-translational modifications, Arch. Biochem. Biophys. 641 (2018) 1–30.
[14] L.B. Wu, H. Yuan, H. Zhou, S.Q. Gao, C.M. Nie, X. Tan, G.B. Wen, Y.W. Lin, An intramolecular disulfide bond designed in myoglobin fine-tunes both protein structure and peroxidase activity, Arch. Biochem. Biophys. 600 (2016) 47–55.
[15] L.L. Yin, H. Yuan, K.J. Du, B. He, S.Q. Gao, G.B. Wen, X. Tan, Y.W. Lin, Regulation of both the structure and function by a de novo designed disulfide bond: a case study of heme proteins in myoglobin, Chem. Commun. (Camb) 54 (2018) 4356–4359.
[16] C. Berndt, C.H. Lillig, A. Holmgren, Thiol-based mechanisms of the thioredoxin and glutaredoxin systems: implications for diseases in the cardiovascular system, Am. J. Physiol. Heart Circ. Physiol. 292 (2007) H1227–H1236.
[17] J. Lu, A. Holmgren, The thioredoxin antioxidant system, Free Radic. Biol. Med. 66 (2014) 75–87.
[18] H. Sies (Ed.), Oxidative Stress: Eustress and Distress, Adademic Press, 2019.
[19] H. Sies, C. Berndt, D.P. Jones, Oxidative stress, Annu. Rev. Biochem. 86 (2017) 715–748.
[20] B. Halliwell, J.M.C. Gutteridge, Free Radicals in Biology & Medicine, Oxford University Press, Oxford, 2015.
[21] Y.-M. Go, D.P. Jones, Redox theory of aging: implications for health and disease, Clin. Sci. (Lond) 131 (2017) 1669–1688.
[22] P. Ghezzi, V. Bonetto, M. Fratelli, Thiol–disulfide balance: from the concept of oxidative stress to that of redox regulation, Antioxidants Redox Signal. 7 (2005) 964–972.
[23] Y.M. Go, D.P. Jones, Redox compartmentalization in eukaryotic cells, Biochim. Biophys. Acta 1780 (2008) 1273–1290.
[24] Y.M. Go, D.P. Jones, Thiol/disulfide redox states in signaling and sensing, Crit. Rev. Biochem. Mol. Biol. 48 (2013) 173–181.
[25] D.P. Jones, Extracellular redox state: refining the definition of oxidative stress in aging, Rejuvenation Res. 9 (2006) 169–181.
[26] K.M. Cook, P.J. Hogg, Post-translational control of protein function by disulfide bond cleavage, Antioxid, Redox Signal 18 (2013) 1987–2015.
[27] M. Anraku, K. Takeuchi, H. Watanabe, D. Kadowaki, K. Kitamura, K. Tomita, A. Kuniyasu, A. Suenaga, T. Maruyama, M. Otagiri, Quantitative analysis of cysteine-34 on the anitioxidative properties of human serum albumin in hemodialysis patients, J. Pharm. Sci. 100 (2011) 3968–3976.
[28] K. Borowczyk, M. Wyszczelska-Rokiel, P. Kubalczyk, R. Głowacki, Simultaneous determination of albumin and low-molecular-mass thiols in plasma by HPLC with UV detection, J. Chromatogr. B 981 (2015) 57–64.
[29] M. Taverna, A.-L. Marie, J.-P. Mira, B. Guidet, Specific antioxidant properties of human serum albumin, Ann. Intensive Care 3 (2013) 4.
[30] J.P. Fabisiak, A. Sedlov, V.E. Kagan, Quantification of oxidative/nitrosative modification of Cys34 in human serum albumin using a fluorescence-based SDS-PAGE assay, Antioxidants Redox Signal. 4 (2002) 855–865.
[31] S. Miyamura, T. Imafuku, M. Anraku, K. Taguchi, K. Yamasaki, Y. Tominaga, H. Maeda, Y. Ishima, H. Watanabe, M. Otagiri, T. Maruyama, Comparison of posttranslational modification and the functional impairment of human serum albumin in commercial preparations, J. Pharm. Sci. 105 (2016) 1043–1049.
[32] A. Bocedi, G. Cattani, L. Stella, R. Massoud, G. Ricci, Thiol disulfide exchange reactions in human serum albumin: the apparent paradox of the redox transitions of Cys34, FEBS J. 285 (2018) 3225–3237.
[33] A. Kawakami, K. Kubota, N. Yamada, U. Tagami, K. Takehana, I. Sonaka, E. Suzuki, K. Hirayama, Identification and characterization of oxidized human serum albumin: a slight structural change impairs its ligand-binding and antioxidant functions, FEBS J. 273 (2006) 3346–3357.
[34] P.M. Ueland, M.A. Mansoor, A.B. Guttormsen, F. Müller, P. Aukrust, H. Refsum, A.M. Svardal, Reduced, oxidized and protein-bound forms of homocysteine and other aminothiols in plasma comprise the redox thiol status—a possible element of the extracellular antioxidant defense system, J. Nutr. 126 (1996) 1281S–1284S.

[35] G. Colombo, G. Aldini, M. Orioli, D. Giustarini, R. Gornati, R. Rossi, R. Colombo, M. Carini, A. Milzani, I. Dalle-Donne, Water-soluble alpha,beta-unsaturated aldehydes of cigarette smoke induce carbonylation of human serum albumin, Antioxidants Redox Signal. 12 (2010) 349–364.

[36] M. Brioschi, E. Gianazza, A. Mallia, B. Zoanni, A. Altomare, A. Martinez Fernandez, P. Agostoni, G. Aldini, C. Banfi, S-thiolation targets albumin in heart failure, Antioxidants (Basel) 9 (2020).

[37] Y. Yano, H. Grigoryan, C. Schiffman, W. Edmands, L. Petrick, K. Hall, T. Whitehead, C. Metayer, S. Dudoit, S. Rappaport, Untargeted adductomics of Cys34 modifications to human serum albumin in newborn dried blood spots, Anal. Bioanal. Chem. 411 (2019) 2351–2362.

[38] K. Nagumo, M. Tanaka, V.T. Chuang, H. Setoyama, H. Watanabe, N. Yamada, K. Kubota, M. Tanaka, K. Matsushita, A. Yoshida, H. Jinnouchi, M. Anraku, D. Kadowaki, Y. Ishima, Y. Sasaki, M. Otagiri, T. Maruyama, Cys34-cysteinylated human serum albumin is a sensitive plasma marker in oxidative stress-related chronic diseases, PLoS One 9 (2014), e85216.

[39] M. Anraku, V.T. Chuang, T. Maruyama, M. Otagiri, Redox properties of serum albumin, Biochim. Biophys. Acta 1830 (2013) 5465–5472.

[40] M. Karimi, M.T. Ignasiak, B. Chan, A.K. Croft, L. Radom, C.H. Schiesser, D. I. Pattison, M.J. Davies, Reactivity of disulfide bonds is markedly affected by structure and environment: implications for protein modification and stability, Sci. Rep. 6 (2016) 38572.

[41] M. Karimi, B. Crossett, S.J. Cordwell, D.I. Pattison, M.J. Davies, Characterization of disulfide (cystine) oxidation by HOCl in a model peptide: evidence for oxygen addition, disulfide bond cleavage and adduct formation with thiols, Free Radic. Biol. Med. 154 (2020) 62–74.

[42] L. Carroll, S. Jiang, J. Irnstorfer, S. Beneyto, M.T. Ignasiak, L.M. Rasmussen, A. Rogowska-Wrzesinska, M.J. Davies, Oxidant-induced glutathionylation at protein disulfide bonds, Free Radic. Biol. Med. 160 (2020) 513–525.

[43] S. Jiang, L. Carroll, M. Mariotti, P. Hägglund, M.J. Davies, Formation of protein cross-links by singlet oxygen-mediated disulfide oxidation, Redox Biol. 41 (2021) 101874.

[44] S. Jiang, L. Carroll, A. Rogowska-Wrzesinska, L.M. Rasmussen, M.J. Davies, Oxidation of disulfide bonds in proteins by singlet oxygen gives rise to glutathionylated proteins, Redox Biol. 38 (2021) 101822.

[45] E.L. Clennan, D.Y. Wang, H.W. Zhang, C.H. Clifton, Photooxidations of sulfenic acid-derivatives. 2. A remarkable solvent effect on the reactions of singlet oxygen with disulfides, Tetrahedron Lett. 35 (1994) 4723–4726.

[46] G.I. Giles, K.M. Tasker, C. Jacob, Oxidation of biological thiols by highly reactive disulfide-S-oxides, Gen. Physiol. Biophys. 21 (2002) 65–72.

[47] K.P. Huang, F.L. Huang, Glutathionylation of proteins by glutathione disulfide S-oxide, Biochem. Pharmacol. 64 (2002) 1049–1056.

[48] P. Nagy, K. Lemma, M.T. Ashby, Reactive sulfur species: kinetics and mechanisms of the reaction of cysteine thiosulfinate ester with cysteine to give cysteine sulfenic acid, J. Org. Chem. 72 (2007) 8838–8846.

[49] D. Butera, T. Wind, A.J. Lay, J. Beck, F.J. Castellino, P.J. Hogg, Characterization of a reduced form of plasma plasminogen as the precursor for angiostatin formation, J. Biol. Chem. 289 (2014) 2992–3000.

[50] T. Ganderton, J.W. Wong, C. Schroeder, P.J. Hogg, Lateral self-association of vWF involves the Cys2431-Cys2453 disulfide/dithiol in the c2 domain, Blood 118 (2011) 5312–5318.

[51] P.M. Ridker, C.H. Hennekens, J.E. Buring, N. Rifai, C-reactive protein and other markers of inflammation in the prediction of cardiovascular disease in women, N. Engl. J. Med. 342 (2000) 836–843.

[52] N.R. Sproston, J.J. Ashworth, Role of C-reactive protein at sites of inflammation and infection, Front. Immunol. 9 (2018) 754.

[53] A.J. Szalai, A. Agrawal, T.J. Greenhough, J.E. Volanakis, C-reactive protein, Immunol. Res. 16 (1997) 127.

[54] M.-Y. Wang, S.-R. Ji, C.-J. Bai, D. El Kebir, H.-Y. Li, J.-M. Shi, W. Zhu, S. Costantino, H.-H. Zhou, L.A. Potempa, A redox switch in C-reactive protein modulates activation of endothelial cells, Faseb. J. 25 (2011) 3186–3196.

[55] M. Boncler, B. Kehrel, R. Szewczyk, E. Stec-Martyna, R. Bednarek, M. Brodde, C. Watala, Oxidation of C-reactive protein by hypochlorous acid leads to the formation of potent platelet activator, Int. J. Biol. Macromol. 107 (2018) 2701–2714.

[56] M.J. Davies, C.L. Hawkins, The role of myeloperoxidase (MPO) in biomolecule modification, chronic inflammation and disease, Antioxidants Redox Signal. 32 (2020) 957–981.

[57] M. Mollenhauer, K. Friedrichs, M. Lange, J. Gesenberg, L. Remane, C. Kerkenpass, J. Krause, J. Schneider, T. Ravekes, M. Maass, M. Halbach, G. Peinkofer, T. Saric, D. Mehrkens, M. Adam, F.G. Deuschl, D. Lau, B. Geertz, K. Manchanda, T. Eschenhagen, L. Kubala, T.K. Rudolph, Y. Wu, W.H.W. Tang, S.L. Hazen, S. Baldus, A. Klinke, V. Rudolph, Myeloperoxidase mediates postischemic arrhythmogenic ventricular remodeling, Circ. Res. 121 (2017) 56–70.

[58] S.J. Nicholls, W.H. Wilson Tang, D. Brennan, M.L. Brennan, S. Mann, S.E. Nissen, S.L. Hazen, Risk prediction with serial myeloperoxidase monitoring in patients with acute chest pain, Clin. Chem. 57 (2011) 1762–1770.

[59] W.H. Tang, Y. Wu, S.J. Nicholls, S.L. Hazen, Plasma myeloperoxidase predicts incident cardiovascular risks in stable patients undergoing medical management for coronary artery disease, Clin. Chem. 57 (2011) 33–39.

[60] N.R. Sproston, M. El Mohtadi, M. Slevin, W. Gilmore, J.J. Ashworth, The effect of C-reactive protein isoforms on nitric oxide production by U937 monocytes/macrophages, Front. Immunol. 9 (2018) 1500.

[61] J.C. Morris, The acid ionization constant of HOCl from 5 ^{o}C to 35 ^{o}C, J. Phys. Chem. 70 (1966) 3798–3805.

[62] D.S. Bohle, B. Hansert, S.C. Paulson, B.D. Smith, Biomimetic synthesis of the putative cytotoxin peroxynitrite, $ONOO^{-}$, and its characterization as a tetramethylammonium salt, J. Am. Chem. Soc. 116 (1994) 7423–7424.

[63] A. Shevchenko, H. Tomas, J. Havli, J.V. Olsen, M. Mann, In-gel digestion for mass spectrometric characterization of proteins and proteomes, Nat. Protoc. 1 (2006) 2856.

[64] F. Wilkinson, W. Helman, A. Ross, Quantum yields for the photosensitized formation of the lowest electronically excited singlet state of molecular oxygen in solution, J. Phys. Chem. 22 (1993) 113–262.

[65] R.W. Redmond, J.N. Gamlin, A compilation of singlet oxygen yields from biologically relevant molecules, Photochem. Photobiol. 70 (1999) 391–475.

[66] M.J. Davies, Singlet oxygen-mediated damage to proteins and its consequences, Biochem. Biophys. Res. Commun. 305 (2003) 761–770.

[67] D.I. Pattison, A.S. Rahmanto, M.J. Davies, Photo-oxidation of proteins, Photochem. Photobiol. Sci. 11 (2012) 38–53.

[68] E.L. Clennan, C. Liao, The hydroperoxysulfonium ylide. An aberration or a ubiquitous intermediate? Tetrahedron 62 (2006) 10724–10728.

[69] E.L. Clennan, D. Wang, C. Clifton, M.F. Chen, Geometry-dependent quenching of singlet oxygen by dialkyl disulfides, J. Am. Chem. Soc. 119 (1997) 9081–9082.

[70] G. Ferrer-Sueta, N. Campolo, M. Trujillo, S. Bartesaghi, S. Carballal, N. Romero, B. Alvarez, R. Radi, Biochemistry of peroxynitrite and protein tyrosine nitration, Chem. Rev. 118 (2018) 1338–1408.

[71] J.R. Kanofsky, Singlet oxygen production by biological systems, Chem. Biol. Interact. 70 (1989) 1–28.

[72] I.E. Kochevar, R.W. Redmond, Photosensitized production of singlet oxygen, Methods Enzymol. 319 (2000) 20–28.

[73] M.J. Davies, The oxidative environment and protein damage, Biochim. Biophys. Acta 1703 (2005) 93–109.

[74] C.L. Hawkins, M.J. Davies, Detection, identification and quantification of oxidative protein modifications, J. Biol. Chem. 294 (2019) 19683–19708.

[75] D.I. Pattison, M.J. Davies, Absolute rate constants for the reaction of hypochlorous acid with protein side chains and peptide bonds, Chem. Res. Toxicol. 14 (2001) 1453–1464.

[76] C. Storkey, M.J. Davies, D.I. Pattison, Reevaluation of the rate constants for the reaction of hypochlorous acid (HOCl) with cysteine, methionine, and peptide derivatives using a new competition kinetic approach, Free Radic. Biol. Med. 73 (2014) 60–66.

[77] C. Storkey, D.I. Pattison, M.T. Ignasiak, C.H. Schiesser, M.J. Davies, Kinetics of reaction of peroxynitrite with selenium- and sulfur-containing compounds: absolute rate constants and assessment of biological significance, Free Radic. Biol. Med. 89 (2015) 1049–1056.

[78] F. Wilkinson, W.P. Helman, A.B. Ross, Rate constants for the decay and reactions of the lowest electronically excited state of molecular oxygen in solution. An expanded and revised compilation, J. Phys. Chem. Ref. Data 24 (1995) 663–1021.

[79] B. Alvarez, R. Radi, Peroxynitrite reactivity with amino acids and proteins, Amino Acids 25 (2003) 295–311.

[80] M.B. Pepys, G.M. Hirschfield, C-reactive protein: a critical update, J. Clin. Invest. 111 (2003) 1805–1812.

[81] W. Ansar, S. Ghosh, C-reactive protein and the biology of disease, Immunol. Res. 56 (2013) 131–142.

[82] D.M. Vigushin, M.B. Pepys, P.N. Hawkins, Metabolic and scintigraphic studies of radioiodinated human C-reactive protein in health and disease, J. Clin. Invest. 91 (1993) 1351–1357.

[83] R.W. Redmond, J.N. Gamlin, A compilation of singlet oxygen yields from biologically relevant molecules, Photochem. Photobiol. 70 (1999) 391–475.

[84] A. Rath, M. Glibowicka, V.G. Nadeau, G. Chen, C.M. Deber, Detergent binding explains anomalous SDS-PAGE migration of membrane proteins, Proc. Natl. Acad. Sci. U.S.A. 106 (2009) 1760–1765A.

[85] Y. Shi, R.A. Mowery, J. Ashley, M. Hentz, A.J. Ramirez, B. Bilgicer, H. Slunt-Brown, D.R. Borchelt, B.F. Shaw, Abnormal SDS-PAGE migration of cytosolic proteins can identify domains and mechanisms that control surfactant binding, Protein Sci. 21 (2012) 1197–1209.

[86] N.H.H. Heegaard, T.J.D. Jorgensen, L. Cheng, C. Schou, M.H. Nissen, O. Trapp, Interconverting conformations of variants of the human amyloidogenic protein beta(2)-microglobulin quantitatively characterized by dynamic capillary electrophoresis and computer simulation, Anal. Chem. 78 (2006) 3667–3673.

[87] T.J.D. Jorgensen, L. Cheng, N.H.H. Heegaard, Mass spectrometric characterization of conformational preludes to beta 2-microglobulin aggregation, Int. J. Mass Spectrom. 268 (2007) 207–216.

[88] M. Trujillo, R. Radi, Peroxynitrite reaction with the reduced and the oxidized forms of lipoic acid: new insights into the reaction of peroxynitrite with thiols, Arch. Biochem. Biophys. 397 (2002) 91–98.

[89] P. Hagglund, M. Mariotti, M.J. Davies, Identification and characterization of protein cross-links induced by oxidative reactions, Expert Rev. Proteomics 18 (2018) 665–681.

[90] F. Leinisch, M. Mariotti, P. Hagglund, M.J. Davies, Structural and functional changes in rnase a originating from tyrosine and histidine cross-linking and oxidation induced by singlet oxygen and peroxyl radicals, Free Radic. Biol. Med. 126 (2018) 73–86.

[91] F. Leinisch, M. Mariotti, M. Rykaer, C. Lopez-Alarcon, P. Hagglund, M.J. Davies, Peroxyl radical- and photo-oxidation of glucose 6-phosphate dehydrogenase generates cross-links and functional changes via oxidation of tyrosine and tryptophan residues, Free Radic. Biol. Med. 112 (2017) 240–252.

[92] L. Carroll, D.I. Pattison, J.B. Davies, R.F. Anderson, C. Lopez-Alarcon, M. J. Davies, Formation and detection of oxidant-generated tryptophan dimers in peptides and proteins, Free Radic. Biol. Med. 113 (2017) 132–142.

[93] D.B. Medinas, F.C. Gozzo, L.F. Santos, A.H. Iglesias, O. Augusto, A ditryptophan cross-link is responsible for the covalent dimerization of human superoxide dismutase 1 during its bicarbonate-dependent peroxidase activity, Free Radic. Biol. Med. 49 (2010) 1046–1053.
[94] V. Paviani, G.T. Galdino, J.N. dos Prazeres, R.F. Queiroz, O. Augusto, Ditryptophan cross-links as novel products of protein oxidation, J. Braz. Chem. Soc. 29 (2018) 925–933.
[95] G. Bhave, C.F. Cummings, R.M. Vanacore, C. Kumagai-Cresse, I.A. Ero-Tolliver, M. Rafi, J.S. Kang, V. Pedchenko, L.I. Fessler, J.H. Fessler, B.G. Hudson, Peroxidasin forms sulfilimine chemical bonds using hypohalous acids in tissue genesis, Nat. Chem. Biol. 8 (2012) 784–790.
[96] C.F. Xu, Y. Chen, L. Yi, T. Brantley, B. Stanley, Z. Sosic, L. Zang, Discovery and characterization of histidine oxidation initiated cross-links in an IgG1 monoclonal antibody, Anal. Chem. 89 (2017) 7915–7923.
[97] D.I. Pattison, C.L. Hawkins, M.J. Davies, What are the plasma targets of the oxidant hypochlorous acid? A kinetic modeling approach, Chem. Res. Toxicol. 22 (2009) 807–817.
[98] M. Trujillo, B. Alvarez, R. Radi, One- and two-electron oxidation of thiols: mechanisms, kinetics and biological fates, Free Radic. Res. 50 (2016) 150–171.
[99] L. Turell, R. Radi, B. Alvarez, The thiol pool in human plasma: the central contribution of albumin to redox processes, Free Radic. Biol. Med. 65C (2013) 244–253.
[100] A. Salvi, P.A. Carrupt, J.M. Mayer, B. Testa, Esterase-like activity of human serum albumin toward prodrug esters of nicotinic acid, Drug Metab. Dispos. 25 (1997) 395–398.
[101] H. Grigoryan, H. Li, A.T. Iavarone, E.R. Williams, S.M. Rappaport, Cys34 adducts of reactive oxygen species in human serum albumin, Chem. Res. Toxicol. 25 (2012) 1633–1642.
[102] A.J. Stewart, C.A. Blindauer, S. Berezenko, D. Sleep, D. Tooth, P.J. Sadler, Role of Tyr84 in controlling the reactivity of Cys34 of human albumin, FEBS J. 272 (2005) 353–362.